Journal Pre-proof

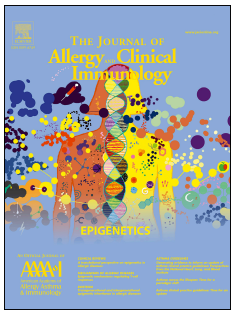

BMP7 aberrantly induced in the psoriatic epidermis instructs inflammation-associated Langerhans cells

Izabela Borek, MSc, René Köffel, PhD, Julia Feichtinger, PhD, Melanie Spies, MD, Elisabeth Glitzner-Zeis, PhD, Mathias Hochgerner, MSc, Tommaso Sconocchia, MSc, Corinna Krump, PhD, Carmen Tam-Amersdorfer, BSc, Christina Passeger, MSc, Theresa Benezeder, MSc, Julia Tittes, MD, Anna Redl, MD, Clemens Painsi, MD, Gerhard G. Thallinger, PhD, Peter Wolf, MD, Georg Stary, MD, Maria Sibilia, PhD, Herbert Strobl, MD

PII: S0091-6749(19)31713-0

DOI: https://doi.org/10.1016/j.jaci.2019.12.011

Reference: YMAI 14312

To appear in: *Journal of Allergy and Clinical Immunology*

Received Date: 28 June 2019

Revised Date: 8 December 2019

Accepted Date: 13 December 2019

Please cite this article as: Borek I, Köffel R, Feichtinger J, Spies M, Glitzner-Zeis E, Hochgerner M, Sconocchia T, Krump C, Tam-Amersdorfer C, Passeger C, Benezeder T, Tittes J, Redl A, Painsi C, Thallinger GG, Wolf P, Stary G, Sibilia M, Strobl H, BMP7 aberrantly induced in the psoriatic epidermis instructs inflammation-associated Langerhans cells, *Journal of Allergy and Clinical Immunology* (2020), doi: https://doi.org/10.1016/j.jaci.2019.12.011.

BMP7 aberrantly induced in the psoriatic epidermis instructs inflammation-associated Langerhans cells

Izabela Borek, MSc[1], René Köffel, PhD[2], Julia Feichtinger, PhD[3], Melanie Spies, MD[1], Elisabeth Glitzner-Zeis, PhD[4], Mathias Hochgerner, MSc[4], Tommaso Sconocchia, MSc[1], Corinna Krump, PhD[1], Carmen Tam-Amersdorfer, BSc[1], Christina Passeger, MSc[1], Theresa Benezeder, MSc[5], Julia Tittes, MD[6], Anna Redl, MD[6], Clemens Painsi, MD[7], Gerhard G Thallinger, PhD[8,9], Peter Wolf, MD[5], Georg Stary, MD[6], Maria Sibilia, PhD[4], Herbert Strobl, MD[1*]

[1]Otto Loewi Research Center, Chair of Immunology and Pathophysiology, Medical University of Graz, Austria.
[2]Institute of Anatomy, University of Bern, Switzerland.
[3]Division of Cell Biology, Histology and Embryology, Gottfried Schatz Research Center for Cell Signaling, Metabolism and Aging, Medical University of Graz, Austria.
[4]Institute of Cancer Research, Department of Internal Medicine I, Medical University of Vienna, Austria.
[5]Department of Dermatology, Medical University of Graz, Austria.
[6]Division of Immunology, Allergy and Infectious Diseases, Department of Dermatology, Medical University of Vienna, Austria.
[7]Department of Dermatology, State Hospital Klagenfurt, Austria.
[8]Institute of Computational Biotechnology, Graz University of Technology, Austria.
[9]OMICS Center Graz, BioTechMed Graz, Austria.

Correspondence

*Herbert Strobl, Otto Loewi Research Center, Chair of Immunology and Pathophysiology, Medical University of Graz, Heinrichstrasse 31a, 8010 Graz, Austria, herbert.strobl@medunigraz.at

Key messages:

- BMP7 instructs proliferating LCs with a psoriatic inflammation-associated phenotype
- The psoriatic epidermal niche is characterized by a BMP7/phospho-Smad1/5/8 signature
- In psoriatic patients reduction in epidermal BMP7 expression is associated with clinical improvement, and BMP signalling promotes psoriatic lesion formation in mice

Capsule summary: BMP signaling is functionally involved in the progression of psoriatic epidermal thickening, and serves as an instructive factor in self-renewal and differentiation of inflammation-associated LCs.

Key words: Langerhans cells, TGF-β signaling, Psoriasis, BMP7

This work was supported by the Austrian Science Fund FWF (W1241) and the Medical University of Graz through the PhD Program Molecular Fundamentals of Inflammation (DK-MOLIN, to HS). Additional funding was obtained by FWF PhD program W1212 (to HS), FWF project P2572 (to HS), BioTechMed Graz (project "secretome", to HS) and by the Austrian Ministry of Science, Research and Economy (HSRSM grant Omics Center Graz, to G.G.T.).

The authors have declared that no conflict of interest exists.

Abbreviations

BG	Birbeck granules
BMP7	bone morphogenetic protein 7
DCs	dendritic cells
IDECs	inflammatory dendritic epidermal cells
KCs	keratinocytes
LCs	Langerhans cells
Nog	noggin
PASI	psoriasis area and severity index
PGN	peptidoglycan
TGF-β1	transforming growth factor beta 1
TLR	tool-like receptor

Abstract

Background: Epidermal hyperplasia represents a morphologic hallmark of psoriatic skin lesions. Langerhans cells (LCs) in the psoriatic epidermis engage with keratinocytes (KCs) in tight physical interactions; moreover, they induce T cell-mediated immune responses critical to psoriasis.

***Objective*:** Epidermal factors in psoriasis pathogenesis remain poorly understood.

***Methods*:** We phenotypically characterized BMP7-LCs vs. TGF-β1-LCs and analyzed their functional properties using flow cytometry, cell kinetic studies, co-culture with CD4 T-cells and cytokine measurements. Furthermore, immunohistology of healthy and psoriatic skin was performed. Additionally, *in vivo* experiments with $Jun^{f/f}JunB^{f/f}K5cre^{ER}$ mice were carried out to assess the role of BMP signaling in psoriatic skin inflammation.

Results: Here we identified a KC-derived signal, i.e. bone morphogenetic protein (BMP) signaling, to promote epidermal changes in psoriasis. Whereas BMP7 is strictly confined to the basal KC layer in the healthy skin, it is expressed at high levels throughout the lesional psoriatic epidermis. BMP7 instructs precursor cells to differentiate into LCs that phenotypically resemble psoriatic LCs. These BMP7-LCs exhibit proliferative activity and increased sensitivity to bacterial stimulation. Moreover, aberrant high BMP signaling in the lesional epidermis is mediated by a KC intrinsic mechanism, as suggested from murine data and clinical outcome after topical anti-psoriatic treatment in human patients.

Conclusion: Our data indicate that available TGF-β family members within the lesional psoriatic epidermis preferentially signal through the canonical BMP signaling cascade to instruct inflammatory-type LCs and to promote psoriatic epidermal changes. Targeting BMP signaling might allow to therapeutically interfere with cutaneous psoriatic manifestations.

Introduction

Langerhans cells (LCs) are a subset of dendritic cells (DCs) populating the epidermis and other squamous epithelia (1). They protect keratinocytes (KCs) from UV light-induced apoptosis (2) and contribute to skin homeostasis by maintaining proliferation of skin resident regulatory T cells (Tregs) (3,4). Psoriatic lesions are marked by epidermal thickening (acanthosis) due to impaired differentiation and enhanced proliferation of KCs (5). The human lesional psoriatic epidermis harbors two subsets of DCs: LCs and epithelial dendritic cells (DCs) that exhibit certain LC characteristics (6). These epidermal DCs are in physical contact with KCs and therefore might play critical roles in psoriasis-associated epidermal changes, as suggested from murine studies (7,8). *Vice versa*, psoriatic KCs might instruct precursors to adopt a disease-associated LC phenotype. Nevertheless, the functional roles of epidermal DCs and LCs remain poorly characterized as most published studies focused on dermal DCs (9). Following an inflammatory insult, endogenous LCs egress from the epidermis and are subsequently replenished from circulating monocytes (10–13), which acquire LC characteristics, but retain certain monocyte features (11). They seem to disappear after the resolution of inflammation and are subsequently replaced by proliferation of residual local LCs (14) or by immigrating non-monocyte, bone marrow-derived precursors (15). The epidermal microenvironment plays a key role in instructing LC differentiation (16), as highlighted by the observations that subsets of LCs from oral mucosa vs epidermis arise from distinct precursors; nevertheless, they exhibit a similar gene expression profile (17). *In vitro* studies revealed that besides monocytes, also human blood $CD1c^+$ DCs and $CD14^+$ dermal cells can differentiate into LCs (18–20). *In vitro*, keratinocyte-derived factors such as TGF-β1 and BMP7 in cooperation with thymic stromal lymphopoietin (TSLP) and Notch ligands promote *in vitro* LC differentiation from human monocytes or monocyte-committed intermediates (21–23). However, unlike monocytes, $CD1c^+$ blood DCs do not require exogenous Notch ligand for LC differentiation (19). Belonging to the TGF-β family, TGF-β1 and BMP7 both signal via BMP type-I receptor ALK3 to induce LC differentiation *in vitro* (24), and TGF-β1 can be replaced by BMP7 for instructing LC differentiation from $CD1c^+$ blood DCs and hematopoietic progenitor cells (19). Conversely, deletion of either TGF-β1, TGF-β1RII (25–27) or TGF-β type I receptor ALK5 (28,29) in differentiated $CD207^+$ cells results in their emigration from the epidermis to the lymph nodes shortly

after birth. Moreover, ALK5 is dispensable for human LC differentiation *in vitro* (24). Whether or how local expression of TGF-β ligands in the healthy and diseased epidermal microenvironment affect LC phenotype and function remains poorly understood. Considering the suspected functional importance of LCs in the maintenance of epidermal homeostasis, a better characterization of TGF-β family signaling in the psoriatic epidermis is of considerable medical relevance. Therefore, we here asked: What are the phenotypic and functional characteristics of BMP7-instructed LCs, and can we find such cells *in vivo* under pathophysiological conditions? We here identified BMP signaling to be functionally involved in the progression of psoriatic epidermal thickening, and to serve as an instructive factor in self-renewal and differentiation of inflammation-associated LCs.

Materials and Methods

In vitro generation of CD34$^+$ progenitor cell-derived LCs, CD14$^+$ monocyte-derived DCs (moDCs) and LCs (moLCs), and CD1c$^+$ blood DCs-derived LCs (CD1c-LCs).

CD34$^+$ cord blood HSCs were expanded for 3 days in serum-free X-vivo^{TM}15 medium (Lonza, Switzerland) supplemented with: 50ng/ml SCF, FLT3-L, TPO each. *In vitro* LCs were generated as previously described (30). In brief, expanded CD34$^+$ cells ($4x10^4$/ml) were cultured for 7 days in serum-free CellGenix® GMP DC medium (CellGenix, Germany) supplemented with: 100ng/ml GM-CSF, 50ng/ml FLT3-L, 20ng/ml SCF, 2.5ng/ml TNFα, and 1ng/ml TGF-β1 or 200ng/ml BMP7. For moDC generation, CD14$^+$ monocytes ($1x10^6$/ml) were cultured for 6 days in RPMI-1640 + 10% FBS (Sigma-Aldrich, USA) supplemented with: 35ng/ml IL-4 and 100ng/ml GM-CSF. For CD1c-LC generation, peripheral blood CD1c$^+$DCs ($5x10^5$/ml) were cultured for 3-4 days in RPMI-1640 + 10% FBS supplemented with: 100ng/ml GM-CSF, and 10ng/ml TGF-β1 or 200ng/ml BMP7. For moLC generation, CD14$^+$ monocytes ($1x10^6$/ml) were cultured for 5 days in Delta-1 coated plates (31) in RPMI-1640 + 10% FBS supplemented with: 100ng/ml GM-CSF, and 10ng/ml TGF-β1 or 200ng/ml BMP7.

Flow cytometry

Flow cytometry staining (extracellular epitopes) was performed as previously described (32). Data were acquired with LSRII instrument (BD Bioscience, USA) and analyzed with FlowJo software (Tree Star, Inc. USA). For the FACS sorting the BD FACS Aria flow cytometer (BD Bioscience, USA) was used. Monoclonal antibodies are listed in the supplementary table 1.

Cytokine measurements

Day 7 CD207$^+$LCs were MACS sorted (purity ≥90%) and activated with 5μg/ml PGN. After 48h supernatants were collected. The proteome profiler human cytokine array kit (R&D Systems, USA) was used according to the manufacturer's instructions. Spot intensity was quantified with ImageLab^{TM} software (BioRad). For the quantitative measurement of cytokines in the supernatants from MLRs Luminex system was used.

Dithranol clinical trial

Paraffin-embedded materials from pre- and post-treatment (4 weeks after therapy completion) biopsy samples were available from six patients (5 men, 1 woman; age range 21-77 years) of a clinical study investigating the effect of topical dithranol in psoriasis. Dithranol study Clinical Trials.gov no.NCT02752672; approval number A23/15, Ethical Committee of the State of Carinthia, Austria.

Statistics

Statistical analysis was performed using 2-tailed *t*-test or one-way ANOVA (corrected with Tukey multiple comparison test) with GraphPad Prism6 software (GraphPad Software Inc.). p-values ≤ 0.05 were considered significant.

Detailed description of cytokines and reagents, cell isolation, preparation of single cell suspension from psoriatic skin biopsies, RNA isolation and gene expression analysis, cytokine measurements, transmission electron microscopy, immunofluorescence and immunohistochemistry, mice, intradermal noggin injections in mice, dorsomorphin treatment, murine skin thickness measurement, and T-cell proliferation assay can be found in the supplemental material.

Results

BMP7-LCs are responsive to TLR2 stimulation

We recently found that BMP7 replaces TGF-β1 in instructing LC differentiation from $CD34^+$ hematopoietic progenitor cells (24). Adding either TGF-β1 or BMP7 to a mix of cytokines in serum-free medium promotes the formation of E-cadherin-mediated clustering $CD1a^+CD207^+$ LCs (Fig. 1A). TGF-β1- and BMP7-generated LCs (termed TGF-β1-LCs and BMP7-LCs, respectively) both exhibit phenotypic characteristics of LCs ($CD1a^+CD207^+CD324^+$ (24)). However, genome-wide microarray analyses of sorted $CD1a^+CD207^+$ cells revealed several differentially expressed genes in BMP7-LCs vs. TGF-β1-LCs (Fig. 1B). Subsequent qRT-PCR analyses showed that both TGF-β1-LCs and BMP7-LCs lack detectable expression of several toll-like receptors (i.e. TLRs 3, 4, 5, 7, 8, 9), as also observed for *ex vivo* isolated LCs (33). However, BMP7-LCs express higher levels of bacterial recognition receptor TLR2 (Fig. 1C, 1D) and lower levels of TLR1, TLR6, as well as lower levels of anti-inflammatory TLR10 (34,35) than TGF-β1-LCs (Fig. 1C). Moreover, TLR2 positivity by BMP7-LCs is correlated with reduced CD207 expression (Fig. 1D). Bacterial ligand peptidoglycan (PGN) was added to TGF-β1-LCs vs. BMP7-LCs to analyze their cytokine/chemokine response to TLR2-mediated stimulation (Fig. 1E). Analyzing a limited panel of cytokines, we previously found that BMP7-LCs indeed exceed TGF-β1-LCs in PGN-induced cytokine production (24). We here confirmed and extended on these observations. BMP7-LCs responded to PGN with increased synthesis of several cytokines (i.e. TNFα, IL6, and GM-CSF) and chemokines (CXCL1, CCL3/4, and CCL1) relative to TGF-β1-LCs (Fig. 1E). Moreover, TGF-β1-LCs equaled BMP7-LCs in their basal and PGN-induced production of IL-8, IL-21, CCL2, ICAM1 and CCL5 (Fig. 1E). To further investigate functional aspects of BMP7-LCs, we performed a mixed lymphocyte reaction (MLR). This analysis showed that BMP7-LCs are not only more potent stimulators of T cell proliferation than TGF-β1-LCs (Fig. S1A), but they also primed naive CD4 T cells towards high production of GM-CSF, TNFα, IL-1β, and IL-2. Inversely, TGF-β1-LCs stimulated CD4 T cells to secrete high levels of anti-inflammatory IL-10 (Fig. S1B).

BMP7 promotes the generation of LCs exhibiting CD1c^{+}CD206^{+} phenotype

Above-mentioned gene array profiling (Fig. 1B) revealed differential expression of several mRNAs encoding cell surface molecules. Subsequent flow cytometry showed that BMP7-LCs express higher levels of CD11c, CD1c, CD206, CD36, CD80, CXCR1 and CX3CR1, and lower levels of Trop2 (TACSTD2) than TGF-β1-LCs (Fig. 2A). Therefore, BMP7-LCs differ from both *in vitro* generated TGF-β1-LCs and *ex vivo* isolated LCs in that they are CD1c^{hi}CD206^{hi}CD36^{hi}TROP2$^{lo/neg}$. Moreover, BMP7-LCs exhibit constitutively active canonical BMP signaling, as evidenced by their significantly higher expression level of pSmad1/5/8, when compared to TGF-β1-LCs (Fig. S2). Given their inflammation-associated characteristics (Fig.1, Fig. S1), we phenotypically compared BMP7-LCs to monocyte-derived DCs (moDCs) known to resemble inflammatory dendritic epidermal cells (IDECs) in eczema/atopic dermatitis lesions (36–39). BMP7-LCs clearly differed from moDCs in parallel analyses (compare Fig. S3 with Fig. 2A). First, moDCs lack LC-associated CD207, CD324/E-cadherin, EpCAM and TACSTD2/TROP2; Second, unlike BMP7-LCs, moDCs express high levels of CD209/DC-SIGN and CD11b (Fig. S3 (40,41)).

LCs generated from peripheral blood precursors are CD206^{+}CD1c^{+}

Murine studies showed that during inflammation LCs develop from monocytes (10,11,13). Recently, human CD1c^{+} blood DCs were identified as candidate LC precursors, since they rapidly (within 72h) differentiate into CD207^{+}CD1a^{+}LCs (19). Whether LCs generated from these cells phenotypically resemble inflammation-associated LCs remains unknown. We purified CD1c^{+} blood DCs from MNCs by first depleting monocytes and B cells, followed by anti-CD1c positive selection. Importantly, CD1c^{+} blood DCs were resolved as a distinct population from CD14^{+} monocytes (Fig. 2B). Both CD1c^{+} blood DCs and CD14^{+} monocytes differentiated into CD206^{+}CD1c^{+}CD36^{+}CD207^{+}CD1a^{+}LCs in both TGF-β1/GM-CSF and BMP7/GM-CSF cultures (Fig. 2C, 2D). Therefore, LCs generated from CD14^{+} monocytes or CD1c^{+} blood DCs exhibit a CD206^{+}CD1c^{+} phenotype, irrespective of whether they are generated in response to TGF-β1 or BMP7.

BMP7-LCs lack detectable Birbeck granules

Birbeck granules (BG) represent a hallmark ultrastructural characteristic of LCs. It was previously shown that a subset of lesional psoriatic epidermal LCs lack detectable BG (37). Moreover, LC maturation has been associated with depletion of BG, due to reduction of the intracellular langerin pool (42). Duplicating previous findings (30,43), TGF-β1-LCs contained numerous intracytoplasmic BG. Conversely, BMP7-LCs lacked BG, despite positivity for CD207.

BMP7-LCs resemble psoriatic LCs and the psoriatic epidermis is marked by BMP7 induction

$CD207^+$ cells from healthy skin are $CD1c^{low/-}CD206^{neg}$. Conversely, the psoriatic epidermis harbors $CD207^+$ cells with phenotypical resemblance to BMP7-LCs as they are also $CD1c^+CD206^+$ (Fig. 3A, 3B). Flow cytometry analysis of cells from lesional biopsies confirmed that $CD207^+$ cells found in psoriatic skin co-express CD1c, CD206 and TLR2, similar to BMP7-LCs (Fig. 3C). We also detected dermal $CD206^+CD1c^+$ cells; however these cells lack CD207 (Fig. 3B). BMP receptors and downstream effectors can be analyzed *in situ*. BMPs bind to the type-II receptor (BMPRII), leading to the recruitment and phosphorylation of a BMP type-I receptor and downstream Smad1/5/8. Strikingly, $CD207^+$LCs in healthy and psoriatic skin are marked by a strong BMPRII expression (Fig. 3D, 3E). As described previously by our group (24), BMP7 expression is confined to the basal/germinal keratinocyte layers, a predominant site of LC residency in healthy human skin (Fig. 4A). In marked contrast, BMP7 is expressed throughout the acanthotic epidermis, and LCs occur scattered in psoriatic lesions (Fig. 4B). Whereas the healthy epidermis exhibits a weak phospho-Smad1/5/8 staining pattern (Fig. 4C), psoriatic LCs and KCs show a strong nuclear accumulation of phospho-Smad1/5/8 (Fig. 4D). JunB is a known psoriasis risk associated gene located on the PSOR6 locus, and JunB expression is downregulated in psoriatic lesional skin (44). Conversely c-Jun expression is enhanced in the basal layer potentially regulating keratinocyte proliferation (45). Tamoxifen (Tx)-induced, epidermal deletion of Jun/JunB in the $Jun^{f/f}JunB^{f/f}$ *K5cre-ER*^{T} mouse model causes a psoriasis-like disease (44), marked by strong lesional epidermal BMP7/phospho-Smad1/5/8 expression (Fig. 4E), duplicating findings in human. Thus, a genetic defect induced in adult KCs (i.e. Jun/JunB deletion) drives psoriatic lesion formation (44) associated with high BMP7 expression. Injection of the BMP antagonist noggin

(nog) is an established *in vivo* experimental approach to study the importance of BMP signaling in skin biology (46–49). Thus, we injected intradermally beads-adsorbed nog (nog) into the ears of *Jun*$^{f/f}$*JunB*$^{f/f}$ *K5cre-ER*^{T} mice 24 h prior to Jun/JunB deletion, and monitored ear swelling for 12 consecutive days (Fig. 4F). Expectedly, as a result of noggin treatment we found diminished pSmad1/5/8 staining intensity in the epidermis (Fig. S4A). While control mice exhibited progressive ear thickening from days 5 onwards, nog injected mice showed significantly reduced ear swelling over the course of the experiment (Fig. 4G, 4H). Histological analysis confirmed decreased epidermal thickening in nog-injected compared to control-injected animals (Fig. 4I, 4J). Furthermore, treatment of developed lesions with topical application of the BMP pathway inhibitor dorsomorphin (targeting type 1 receptors Alk2, 3 and 6) resulted in decreased ear swelling in comparison to the control treated mice (Fig. S4B). In aggregate, these murine and human data demonstrate that the lesional psoriatic epidermis is characterized by aberrant high BMP7/phospho-Smad1/5/8 expression, and that BMP7-LCs phenotypically resemble lesional LCs (CD207^{+}CD206^{+}CD1c^{+}).

BMP7 supplementation is associated with proliferation of CD207^{+} LCs

LC numbers gradually increase during skin development, and CD207^{+}LCs undergo self -renewal *in vivo* (14). However, the epidermal factors promoting LC proliferation remain unknown. Interestingly, BMP7-supplemented cultures showed vigorous proliferation, increased total cellularity and elevated numbers of LCs, relative to TGF-β1-supplemented cultures (Fig. 5A, 5B); We detected mitotic Ki67^{+} cells among CD207^{+}LCs, with percentages Ki67^{+} cells being much higher for BMP7-LC than for TGF-β-LCs (Fig. 5C, 5D). Therefore, BMP7 signaling allows active cycling of *in vitro* generated LCs. In the healthy adult epidermis, BMP7 expression is confined to basal KCs (Fig. 4A; 5E, left; (24)). We analysed whether Ki67^{+}LCs, known to occur in the healthy epidermis (14), co-localize with BMP7^{+}KCs *in situ*. Indeed, Ki67^{+}LCs and Ki67^{+}KCs are confined to the BMP7^{+} epidermal layers (Fig. 5E, left, 5G). In comparison, higher numbers of Ki67^{+}CD207^{+}LCs and Ki67^{+}KC are observed in the lesional BMP7^{hi} psoriatic epidermis (Fig. 5E right, 5F). In inflamed skin the confinement of proliferating cells to the basal epidermal layer was lost, and proliferating LCs and KCs could be found throughout the enlarged BMP7^{hi} epidermis (Fig. 5E, right; model in Fig. S5).

Canonical TGF-β1-ALK5 signaling inhibits phenotypic characteristics of BMP7-LCs

In healthy human epidermis, TGF-β1 is expressed in supra-basal/outer KC layers; conversely, BMP7 is confined to basal KCs (Fig. 4A; 5E (24)). Canonical TGF-β1-ALK5 signaling is required to retain LCs in a non-activated state *in situ* (27). TGF-β1 co-activates both ALK5 and ALK3 (Fig. 6A), the latter being required for TGF-β1-dependent LC differentiation *in vitro* (24); conversely, BMP7 signals through ALK3 but not ALK5 (Fig. 6A; (24,50,51)). BMP7-LCs and lesional psoriatic LCs are $CD1c^{+}/CD206^{+}$, whereas TGF-β1-LCs and steady-state LCs lack these markers (Fig. 2A, 3A). We therefore investigated whether active ALK5 signaling represses CD1c and CD206. Indeed, short-term (48 h) stimulation of BMP7-LCs with TGF-β1 downregulated both CD1c and CD206 (Fig. 6B, lower panel). We performed an inversed experiment to validate these findings. Pharmacological inhibition of the ALK5 receptor in TGF-β1-LC cultures dose-dependently led to the re-establishment of the $CD1c^{+}CD206^{+}$ LC phenotype (Fig. 6C). Together these data revealed that selective ALK3 activation by BMP7 induces a $CD1c^{+}CD206^{+}$ LC phenotype, whereas co-activation of the canonical TGF-β1-ALK5 cascade represses CD1c and CD206.

Topical treatment of psoriatic lesions diminishes BMP7 expression

Topical treatment of psoriatic lesions with dithranol (anthralin) inhibits KC proliferation (52), and our murine data indicate a KC-intrinsic mechanism of BMP7 induction during the onset of psoriatic-like epidermal hyperplasia (Fig. 4E). We monitored BMP7 expression in serial lesional skin biopsies before and after dithranol treatment of psoriatic patients (n=6). Expectedly, before treatment BMP7 was expressed throughout the lesional epidermis (Fig 7A). Four weeks after treatment initiation, BMP7 staining intensity was markedly reduced with only basal KC layers staining positive for BMP7 (Fig. 7A), similarly as observed in the healthy skin (Fig. 4A). The clinical status of the patients was monitored using the psoriasis area and severity index (PASI) score. Out of six analysed patients, after treatment, four exhibited a substantial reduction in BMP7 staining intensity. (Fig. 7A, diagram). Correlation analysis revealed a positive correlation between BMP7 reduction and PASI score reduction (Fig. 7B). All four patients with strong BMP7 reduction also had strong reduction in PASI

score. Conversely, the patient who had no BMP7 decrease also had no PASI score improvement after the completion of the therapy (Fig. 7B).

Discussion

Cutaneous psoriatic lesions are characterized by epidermal hyperplasia and are populated by bone marrow-derived epidermal LC-like cells (6,53). However, the epidermal factors instructing LC differentiation under normal and diseased conditions are poorly defined. While we previously showed that BMP7 is confined to the basal KC layer in the healthy epidermis (24), we here demonstrated that BMP7 and associated downstream BMP signaling components (i.e. phospho-SMAD1/5/8) are highly expressed throughout the enlarged psoriatic epidermis. Using gene profiling, we further showed that BMP7 induces the generation of $CD1c^{+}CD206^{+}$LCs *in vitro*, phenotypically mimicking psoriasis-associated LC-like cells. Moreover, a substantial fraction of *in vitro* generated BMP7-LCs exhibited mitotic activity, similarly as observed for psoriatic LCs *in situ*. We previously showed that ~40% of $CD207^{+}$LCs in murine psoriatic lesions are of bone marrow origin, and these cells exceeded host-derived LCs in mitotic activity (7). Extending on these analyses we here showed that induction of psoriatic lesions by genetic targeting of adult KCs in $Jun^{f/f}JunB^{f/f}$ K5cre-ER^{T} mice also causes a $BMP7^{hi}$/phospho-$SMAD1/5/8^{hi}$ phenotype, indicating a KC-intrinsic mechanism for BMP7 induction. Together these data suggest a key role for epidermal KC-derived BMP7 in instructing LC differentiation from bone marrow-derived precursors in psoriatic lesions (see hypothetical model in Fig. S5). Furthermore, we demonstrated that lesional BMP7 is strongly diminished upon dithranol treatment of psoriatic patients, and that epidermal BMP7 reduction correlates with clinical improvement. Moreover, injection of BMP antagonist noggin in $Jun^{f/f}JunB^{f/f}$ K5cre-ER^{T} mice led to the reduction in epidermal thickening, indicating involvement of BMP signaling in psoriatic lesion formation.

Our phospho-Smad1/5/8 stainings support that the BMP pathway is aberrantly activated in the psoriatic epidermis. However, despite high expression of BMP7 protein throughout the lesional KCs, BMP7 might not be the only BMP family member expressed in the psoriatic epidermis. Interestingly, psoriatic epidermal lesions were previously shown to exhibit diminished canonical TGF-β signaling, as evidenced by decreased levels of TGF-β type-I receptor ALK5, TGF-βR type-II and phospho-SMAD2/3 (54,55). Moreover, TGF-β2 and TGF-β3 (54,56) are downregulated and inhibitory SMAD7 is induced in the psoriatic epidermis (57). We here showed that the inhibition of ALK5 signaling

(canonical TGF-β1 signaling) in TGF-β1-LC cultures results in the generation of CD1c^{hi}CD206^{hi} LCs (mimicking lesional LCs). Inversely, adding TGF-β1 to BMP7-LC cultures led to the repression of CD1c and CD206. In line with impairment of canonical TGF-β1 signaling in inflammation, Bobr et. al. demonstrated that a portion of murine LCs stain positive for phospho-SMAD2/3 (downstream of TGF-β1-ALK5) in normal but not in inflamed skin (27).

A side-by-side comparison revealed that BMP7-supplemented LC cultures give rise to much higher numbers of human LCs compared to TGF-β1-supplemented cultures. Our data suggest a sequential protocol for the generation of high numbers of LCs from human progenitor cells (i.e. BMP7 followed by TGF-β1) in defined serum-free media for cell therapy-oriented studies. We showed that high percentages of *in vitro* generated CD207^{+}BMP7-LCs are Ki67^{+}, indicating that BMP7-ALK3 signaling facilitates LC cycling. In line with this, the type-II BMP receptor BMPR2 is strongly expressed by LCs *in situ*, and marks LCs in epidermal immunohistology. Consistent with a role of BMP7 in facilitating LC cycling, we observed that Ki67^{+}LCs, known to reside in the healthy epidermis (14,58), are confined to the BMP7^{+}KC layers. Moreover, Ki-67^{+}LCs occurred abundantly and spatially scattered throughout the BMP7^{hi} human psoriatic epidermis. Since lesional psoriatic LCs undergo physical clustering with T cells (9), BMP7 might be critically involved in this process.

During ontogeny LC precursors within the epidermal niche are first exposed to BMP7 followed by TGF-β1 (24,59). TGF-β1-ALK5 signaling enables LCs to remain in their non-activated state, a model directly supported by murine ALK5 (29) and TGF-βRII (26) knock-out studies. Moreover, sequential BMP7/TGF-β1 signaling was shown to instruct murine mucosal LCs differentiation (60); reviewed in: (61). Notably, supernatants of cultured keratinocytes (pre-stimulated or not with IL-17 and TNFα) failed to replace exogenous BMP7 for the promotion of LC differentiation from CD34^{+} cells (unpublished observation). Therefore, cell contact-dependent mechanisms might be required for these effects, e.g. enabling BMP7 processing.

Freshly isolated human LCs were shown to lack detectable TLR4 and to express low or undetectable TLR5 and TLR2 (46,62,63). Van der Aar et al. (63) previously showed that these bacterial recognition receptors are repressed upon TGF-β1 stimulation of monocytes undergoing moLC differentiation and that dermal DCs express these TLRs. Consistently, we here showed that TGF-β1-LCs lack detectable TLR4, TLR5 and TLR2. Moreover, *in vitro* generated CD34^{+} cell-

derived LCs in our study resembled *ex vivo* isolated LCs in detectable expression of TLR1, TLR6 (33,63) and TLR10 (33), as well as in low/non-detectable TLR7 and TLR8 (33). However, inconsistent data have been published regarded the expression of TLR7/9/10 by *ex vivo* isolated LCs (33,62,63). Notably, while TLR3 is expressed by LCs and moLCs (63), we failed to detect TLR3 in $CD34^+$ cell-derived LCs. Whether these differences are inherent to the specific culture models studied remains to be analyzed. We showed here using flow cytometry that BMP7-LCs are $TLR2^+$, whereas TGF-β1-LCs lack detectable TLR2. Moreover, TGF-β1-LCs exceeded BMP7-LCs in levels of TLR10mRNA expression. Interestingly, TLR10 is regarded as the only known inhibitory receptor within the TLR family (recently reviewed in: (64)). TLR10 is able to homodimerize and heterodimerize with TLR1 and TLR2. Elevated TLR2 and diminished TLR10, observed in BMP7-LCs relative to TGF-β1-LCs, might thus contribute to the here observed more potent cytokine production of the former in response to PGN stimulation. It will be interesting to further analyze whether TLR10 is expressed by *in vivo* LCs and if so, whether lesional psoriatic LCs exhibit diminished levels of TLR10. It is interesting to speculate that an inverse expression of TLR2/TLR10 might sensitize LCs from lesional psoriatic skin to gram positive bacteria such as Staphylococcus aureus. In line with this possibility, we detected substantial levels of TLR2 on LCs from lesional psoriatic skin. Consistently, PGN-stimulated BMP7-LCs produced higher levels of several inflammatory mediators (e.g.: IL6, TNFα, CXCL1, CCL3/4) relative to TGF-β1-LCs. Our observations are consistent with the demonstration that TLR2 stimulated LCs are potent inducers of Th17 polarization, highlighting the importance of TLR2 in immune responses in inflamed skin (65). Future studies are required to analyze *in vitro* generated LCs for additional cytokines such as IL-22 and IL-23 known to be involved in psoriasis. Moreover, intracellular cytokine staining needs to be performed to determine the cellular origin of the cytokines measured in the supernatants of LC-T cells co-cultures.

$CD207^+$ BMP7-LCs phenotypically resemble LCs found in lesional psoriatic skin in that these cells are also $CD1c^+CD206^+$. Similarly, LCs generated *in vitro* from monocytes or from peripheral blood $CD1c^+$ DCs express CD1c and CD206, consistent with the concept that these cells may develop into LCs during inflammation (reviewed in: (66)). A monocyte origination of LCs is also evident from studies on their development from $CD34^+$ cells *in vitro*. Monocyte intermediates which arise in these cultures have to lose expression of the monocyte identity factor KLF4, in order to differentiate into

LCs (67). In conclusion, our data are consistent with a model whereby monocytes immigrate to the psoriatic epidermis and there differentiate into $CD207^{+}CD1a^{+}CD1c^{+}CD206^{+}$ LCs. It has been previously shown that in psoriasis CD206 is expressed by a subset of $CD1a^{+}$ epidermal cells (37). Whether human inflammation-associated $CD207^{+}CD1c^{+}CD206^{+}$ LC arise from myeloid progenitor cells, $CD14^{+}$ monocytes or $CD1c^{+}$ blood DC remains to be studied. In this context it is interesting to note that BMP7-LCs phenotypically differed from moDCs, previously shown to resemble atopic dermatitis-associated IDECs (36–39).

Our results demonstrated, that *in vitro* BMP7-LCs express higher levels of several pro-inflammatory genes and exhibit more potent T cell stimulatory capacity than TGF-β1-LCs. This is consistent with the observation that CD1a on LCs facilitates psoriatic skin inflammation both in patients and the murine system (68). However, a regulatory function of these cells *in vivo* cannot be ruled out, considering previously demonstrated regulatory properties of semi-mature or even mature DCs (69); recently reviewed in: (70). With regards to a possible function of psoriatic inflammation-associated LCs, we previously showed that LCs are dispensable for the induction phase of psoriatic lesions in $Jun^{f/f}JunB^{f/f}$ K5cre-ER^{T} mice; however they exerted an immune-regulatory function in chronic lesions (7). Despite our here presented observations that murine lesions in these mice are also $BMP7^{hi}$/p-SMAD1/5/8^{hi}, a direct translation of these findings to the human system must take into account major species differences; recently reviewed in: (70).

We showed that TGF-β1 stimulation represses CD1c and CD206 expression in LCs generated in response to BMP7. It will be interesting to perform therapy-oriented *in vivo* studies addressing whether bone marrow-derived psoriatic LCs might differentiate further into steady-state-like LCs during the resolution phase of cutaneous psoriatic lesions, and whether this process is driven or can be augmented by TGF-β-ALK5 signaling. Moreover, future studies are required to address the molecular mechanism of enhanced BMP7 expression in psoriatic lesions. Among several factors, high BMP7 levels throughout the epidermal psoriatic lesions might be due to the expansion of basal keratinocytes or enhanced processing of BMP7 precursor molecules.

In conclusion, our data indicate that available TGF-β family members within psoriatic epidermal lesions preferentially activate the BMP signaling cascade, leading to the generation of

proliferative, inflammation-associated LCs. Therapeutically targeting of this pathway, or restoration of canonical TGF-β signaling, might allow for interfering with cutaneous psoriatic lesion formation.

.

Acknowledgments

We thank E. Schwarzenberger for cell preparation and technical assistance, T. Brossmann for PCR mice genotyping and sample embedding, I. Fedorenko for technical assistance in EM-sample preparation, and T. Bauer for designing the graphical abstract.

References

1. Heath WR, Carbone FR. The skin-resident and migratory immune system in steady state and memory: Innate lymphocytes, dendritic cells and T cells. Nat Immunol. 2013;14(10):978–85.
2. Hatakeyama M, Fukunaga A, Washio K, Taguchi K, Oda Y, Ogura K, et al. Anti-Inflammatory Role of Langerhans Cells and Apoptotic Keratinocytes in Ultraviolet-B–Induced Cutaneous Inflammation. J Immunol. 2017;199(8):2937–47.
3. Seneschal J, Clark RA, Gehad A, Baecher-Allan CM, Kupper TS. Human Epidermal Langerhans Cells Maintain Immune Homeostasis in Skin by Activating Skin Resident Regulatory T Cells. Immunity. 2012;36(5):873–84.
4. Kitashima DY, Kobayashi T, Woodring T, Idouchi K, Doebel T, Voisin B, et al. Langerhans Cells Prevent Autoimmunity via Expansion of Keratinocyte Antigen-Specific Regulatory T Cells. EBioMedicine. 2018;27:293–303.
5. Lowes MA, Suarez-Farinas M, Krueger JG. Immunology of Psoriasis. Annu Rev Immunol. 2014;32:227–55.
6. Martini E, Wikén M, Cheuk S, Gallais Sérézal I, Baharom F, Ståhle M, et al. Dynamic Changes in Resident and Infiltrating Epidermal Dendritic Cells in Active and Resolved Psoriasis. J Invest Dermatol. 2017;137(4):865–73.
7. Glitzner E, Korosec A, Brunner PM, Drobits B, Amberg N, Schonthaler HB, et al. Specific roles for dendritic cell subsets during initiation and progression of psoriasis. EMBO Mol Med. 2014;6(10):1312–27.
8. Terhorst D, Chelbi R, Wohn C, Malosse C, Tamoutounour S, Jorquera A, et al. Dynamics and Transcriptomics of Skin Dendritic Cells and Macrophages in an Imiquimod-Induced, Biphasic Mouse Model of Psoriasis. J Immunol. 2015;195(10):4953–61.
9. Eidsmo L, Martini E. Human Langerhans cells with pro-inflammatory features relocate within psoriasis lesions. Front Immunol. 2018;9(FEB):1–8.
10. Ginhoux F, Tacke F, Angeli V, Bogunovic M, Loubeau M, Dai XM, et al. Langerhans cells arise from monocytes in vivo. Nat Immunol. 2006;7(3):265–73.
11. Sere K, Baek JH, Ober-Blobaum J, Muller-Newen G, Tacke F, Yokota Y, et al. Two Distinct

Types of Langerhans Cells Populate the Skin during Steady State and Inflammation. Immunity. 2012;37(5):905–16.

12. Chopin M, Seillet C, Chevrier S, Wu L, Wang H, Morse 3rd HC, et al. Langerhans cells are generated by two distinct PU.1-dependent transcriptional networks. J Exp Med. 2013;210(13):2967–80.

13. Singh TP, Zhang HH, Borek I, Wolf P, Hedrick MN, Singh SP, et al. Monocyte-derived inflammatory Langerhans cells and dermal dendritic cells mediate psoriasis-like inflammation. Nat Commun. 2016;7(May):1–18.

14. Chorro L, Sarde A, Li M, Woollard KJ, Chambon P, Malissen B, et al. Langerhans cell (LC) proliferation mediates neonatal development, homeostasis, and inflammation-associated expansion of the epidermal LC network. J Exp Med. 2009;206(13):3089–100.

15. Mende I, Karsunky H, Weissman IL, Engleman EG, Merad M. Flk2+ myeloid progenitors are the main source of Langerhans cells. Blood. 2006;107(4):1383–90.

16. Schuster C, Mildner M, Mairhofer M, Bauer W, Fiala C, Prior M, et al. Human embryonic epidermis contains a diverse Langerhans cell precursor pool. Development. 2014;141(4):807–15.

17. Capucha T, Mizraji G, Segev H, Blecher-Gonen R, Winter D, Khalaileh A, et al. Distinct Murine Mucosal Langerhans Cell Subsets Develop from Pre-dendritic Cells and Monocytes. Immunity. 2015;43(2):369–81.

18. Martínez-Cingolani C, Grandclaudon M, Jeanmougin M, Jouve M, Zollinger R, Soumelis V. Human blood BDCA-1 dendritic cells differentiate into Langerhans-like cells with thymic stromal lymphopoietin and TGF-β. Blood. 2014;124(15):2411–20.

19. Milne P, Bigley V, Gunawan M, Haniffa M, Collin M. CD1c 1 blood dendritic cells have Langerhans cell potential. Blood. 2015;125(3):470–4.

20. Larregina AT, Morelli AE, Spencer LA, Logar AJ, Watkins SC, Thomson AW, et al. Dermal-resident CD14+cells differentiate into Langerhans cells. Nat Immunol. 2001;2(12):1151–8.

21. Hoshino N, Katayama N, Shibasaki T, Ohishi K, Nishioka J, Masuya M, et al. A novel role for Notch ligand Delta-1 as a regulator of human Langerhans cell development from blood monocytes. J Leukoc Biol. 2005;78(4):921–9.

22. Jurkin J, Krump C, Köffel R, Fieber C, Schuster C, Brunner PM, et al. Human skin dendritic cell fate is differentially regulated by the monocyte identity factor Kruppel-like factor 4 during steady state and inflammation. J Allergy Clin Immunol. 2017;139(6).

23. Strobl H, Krump C, Borek I. Micro-environmental signals directing human epidermal Langerhans cell differentiation. Semin Cell Dev Biol. 2018;S1084-9521(17):30350–6.

24. Yasmin N, Bauer T, Modak M, Wagner K, Schuster C, Köffel R, et al. Identification of bone morphogenetic protein 7 (BMP7) as an instructive factor for human epidermal Langerhans cell differentiation. J Exp Med. 2013;210(12):2597–610.

25. Borkowski TA, Letterio JJ, Farr AG, Udey MC. A role for endogenous transforming growth factor beta 1 in Langerhans cell biology: the skin of transforming growth factor beta 1 null mice is devoid of epidermal Langerhans cells. J Exp Med. 1996;184(6):2417–22.

26. Kaplan DH, Li MO, Jenison MC, Shlomchik WD, Flavell RA, Shlomchik MJ. Autocrine/paracrine TGFbeta1 is required for the development of epidermal Langerhans cells. J Exp Med. 2007;204(11):2545–52.

27. Bobr A, Igyarto BZ, Haley KM, Li MO, Flavell RA, Kaplan DH. Autocrine / paracrine TGF- β 1 inhibits Langerhans cell migration. Proc Natl Acad Sci U S A. 2012;109(26):10492–7.

28. Kel JM, Girard-Madoux MJH, Reizis B, Clausen BE. TGF- Is Required To Maintain the Pool of Immature Langerhans Cells in the Epidermis. J Immunol. 2010;185(6):3248–55.

29. Zahner SP, Kel JM, Martina CAE, Brouwers-Haspels I, van Roon MA, Clausen BE. Conditional Deletion of TGF-βR1 Using Langerin-Cre Mice Results in Langerhans Cell Deficiency and Reduced Contact Hypersensitivity. J Immunol. 2011;187(10):5069–76.

30. Strobl H, Riedl E, Scheinecker C, Bello-Fernandez C, Pickl WF, Rappersberger K, et al. TGF-beta 1 promotes in vitro development of dendritic cells from CD34+ hemopoietic progenitors. J Immunol. 1996;157(4):1499–507.

31. Varnum-Finney B, Wu L, Yu M, Brashem-Stein C, Staats S, Flowers D, et al. Immobilization of Notch ligand, Delta-1, is required for induction of notch signaling. J Cell Sci. 2000;113 Pt 23:4313–8.

32. Platzer B, Jörgl A, Taschner S, Höcher B, Strobl H, Platzer B, et al. RelB regulates human dendritic cell subset development by promoting monocyte intermediates. Blood.

2014;104(12):3655–63.

33. Flacher V, Bouschbacher M, Verronese E, Massacrier C, Sisirak V, Berthier-Vergnes O, et al. Human Langerhans Cells Express a Specific TLR Profile and Differentially Respond to Viruses and Gram-Positive Bacteria. J Immunol. 2006;177(11):7959–67.

34. Oosting M, Cheng S-C, Bolscher JM, Vestering-Stenger R, Plantinga TS, Verschueren IC, et al. Human TLR10 is an anti-inflammatory pattern-recognition receptor. Proc Natl Acad Sci. 2014;111(42):E4478–84.

35. Jiang S, Li X, Hess NJ, Guan Y, Tapping RI. TLR10 Is a Negative Regulator of Both MyD88-Dependent and -Independent TLR Signaling. J Immunol. 2016;196(9):3834–41.

36. Wollenberg A, Kraft S, Hanau D, Bieber T. Immunomorphological and ultrastructural characterization of Langerhans cells and a novel, inflammatory dendritic epidermal cell (IDEC) population in lesional skin of atopic eczema. J Invest Dermatol. 1996;106(3):446–53.

37. Wollenberg A, Mommaas M, Oppel T, Schottdorf E-M, Günther S, Moderer M. Expression and function of the mannose receptor CD206 on epidermal dendritic cells in inflammatory skin diseases. J Invest Dermatol. 2002;118:327–34.

38. Novak N, Kraft S, Haberstok J, Geiger E, Allam P, Bieber T. A reducing microenvironment leads to the generation of FcεRIhighinflammatory dendritic epidermal cells (IDEC). J Invest Dermatol. 2002;119(4):842–9.

39. Dijkstra D, Stark H, Chazot PL, Shenton FC, Leurs R, Werfel T, et al. Human Inflammatory Dendritic Epidermal Cells Express a Functional Histamine H4 Receptor. J Invest Dermatol. 2008;128:1696–703.

40. Relloso M, Puig-Kroger A, Pello OM, Rodriguez-Fernandez JL, de la Rosa G, Longo N, et al. DC-SIGN (CD209) Expression Is IL-4 Dependent and Is Negatively Regulated by IFN, TGF- , and Anti-Inflammatory Agents. J Immunol. 2002;168(6):2634–43.

41. Plantinga M, Guilliams M, Vanheerswynghels M, Deswarte K, Branco-Madeira F, Toussaint W, et al. Conventional and Monocyte-Derived CD11b+Dendritic Cells Initiate and Maintain T Helper 2 Cell-Mediated Immunity to House Dust Mite Allergen. Immunity. 2013;38(2):322–35.

42. Mc Dermott R, Ziylan U, Spehner D, Bausinger H, Lipsker D, Mommaas M, et al. Birbeck

granules are subdomains of endosomal recycling compartment in human epidermal langerhans cells, which form where langerin accumulates. Mol Biol Cell. 2002;13:317–35.

43. Caux C, Massacrier C, Dubois B, Valladeau J, Dezutter-Dambuyant C, Durand I, et al. Respective involvement of TGF-β and IL-4 in the development of Langerhans cells and non-Langerhans dendritic cells from CD34+progenitors. J Leukoc Biol. 1999;66(5):781–91.

44. Zenz R, Eferl R, Kenner L, Florin L, Hummerich L, Mehic D, et al. Psoriasis-like skin disease and arthritis caused by inducible epidermal deletion of Jun proteins. Nature. 2005;437(7057):369–75.

45. Mehic D, Bakiri L, Ghannadan M, Wagner EF, Tschachler E. Fos and Jun proteins are specifically expressed during differentiation of human keratinocytes. J Invest Dermatol. 2005;124(1):212–20.

46. Plikus M V, Mayer J, Cruz D De, Baker RE, Maini PK, Maxson R, et al. Cyclic dermal BMP signaling regulates stem cell activation during hair regeneration. Nature. 2008;451(7176):340–4.

47. Greco V, Chen T, Rendl M, Schober M, Pasolli HA, Stokes N, et al. A Two-Step Mechanism for Stem Cell Activation during Hair Regeneration. Cell. 2009;4(2):155–69.

48. Oshimori N, Fuchs E. Paracrin TGF-beta signaling Counterbalance BMP-mediated Repression in Hair Folicle Stem Cell Activation. Cell Stem Cell. 2012;10(1):63–75.

49. Lee J, Kang S, Lilja KC, Colletier KJ, Scheitz CJF, Zhang Y V, et al. Signalling couples hair follicle stem cell quiescence with reduced histone H3 K4/K9/K27me3 for proper tissue homeostasis. Nat Commun. 2016;7:11278.

50. Daly AC, Randall RA, Hill CS. Transforming Growth Factor beta-Induced Smad1/5 Phosphorylation in Epithelial Cells Is Mediated by Novel Receptor Complexes and Is Essential for Anchorage-Independent Growth. Mol Cell Biol. 2008;28(22):6889–902.

51. Miyazono K, Kamiya Y, Morikawa M. Bone morphogenetic protein receptor and signal transduction. J Biochem. 2010;147(1):35–51.

52. Holstein J, Fehrenbacher B, Brück J, Müller-Hermelink E, Schäfer I, Carevic M, et al. Anthralin modulates the expression pattern of cytokeratins and antimicrobial peptides by psoriatic keratinocytes. J Dermatol Sci. 2017;87(3):236–45.

53. Korenfeld D, Gorvel L, Munk A, Man J, Schaffer A, Tung T, et al. A type of human skin dendritic cell marked by CD5 is associated with the development of inflammatory skin disease. J Clin Invest. 2017;2(18):e96101.

54. Doi H, Shibata MA, Kiyokane K, Otsuki Y. Downregulation of TGFβ isoforms and their receptors contributes to keratinocyte hyperproliferation in psoriasis vulgaris. J Dermatol Sci. 2003;33(1):7–16.

55. Jiang M, Sun Z, Dang E, Li B, Fang H, Li J, et al. TGFβ/SMAD/microRNA-486-3p Signaling Axis Mediates Keratin 17 Expression and Keratinocyte Hyperproliferation in Psoriasis. J Invest Dermatol. 2017;137(10):2177–86.

56. Wataya-Kaneda M, Hashimoto K, Kato M, Miyazono K, Yoshikawa K. Differential localization of TGF-beta-precursor isotypes in psoriatic human skin. J Dermatol Sci. 1996;11(3):183–8.

57. Di Fusco D, Laudisi F, Dinallo V, Monteleone I, Di Grazia A, Marafini I, et al. Smad7 positively regulates keratinocyte proliferation in psoriasis. Br J Dermatol. 2017;177(6):1633–43.

58. Kanitakis J, Morelon E, Petruzzo P, Badet L, Dubernard JM. Self-renewal capacity of human epidermal Langerhans cells: Observations made on a composite tissue allograft. Exp Dermatol. 2011;20(2):145–6.

59. Schuster C, Vaculik C, Fiala C, Meindl S, Brandt O, Imhof M, et al. HLA-DR+ leukocytes acquire CD1 antigens in embryonic and fetal human skin and contain functional antigen-presenting cells. J Exp Med. 2009;206(1):169–81.

60. Capucha T, Koren N, Nassar M, Heyman O, Nir T, Levy M, et al. Sequential BMP7/TGF-β1 signaling and microbiota instruct mucosal Langerhans cell differentiation. J Exp Med. 2018;215(2):481–500.

61. Hovav AH. Mucosal and Skin Langerhans Cells – Nurture Calls. Trends Immunol. 2018;39(10):788–800.

62. Peiser M, Koeck J, Kirschning CJ, Wittig B, Wanner R. Human Langerhans cells selectively activated via Toll-like receptor 2 agonists acquire migratory and CD4 + T cell stimulatory capacity . J Leukoc Biol. 2008;83(5):1118–27.

63. van der Aar AMG, Sylva-Steenland RMR, Bos JD, Kapsenberg ML, de Jong EC, Teunissen MBM. Cutting Edge: Loss of TLR2, TLR4, and TLR5 on Langerhans Cells Abolishes Bacterial Recognition. J Immunol. 2007;178(4):1986–90.

64. Nagashima H, Yamaoka Y. Importance of toll-like receptors in pro-inflammatory and anti-inflammatory responses by helicobacter pylori infection. Curr Top Microbiol Immunol. 2019;421:139–58.

65. Aliahmadi E, Gramlich R, Grützkau A, Hitzler M, Krüger M, Baumgrass R, et al. TLR2-activated human langerhans cells promote Th17 polarization via IL-1β, TGF-β and IL-23. Eur J Immunol. 2009;39(5):1221–30.

66. Collin M, Bigley V. Human dendritic cell subsets: an update. Immunology. 2018;154(1):3–20.

67. Jurkin J, Krump C, Köffel R, Fieber C, Schuster C, Brunner PM, et al. Human skin dendritic cell fate is differentially regulated by the monocyte identity factor Kruppel-like factor 4 during steady state and inflammation. J Allergy Clin Immunol. 2017;139(6):1873-1884.e10.

68. Kim JH, Hu Y, Yongqing T, Kim J, Hughes VA, Le Nours J, et al. CD1a on Langerhans cells controls inflammatory skin disease. Nat Immunol. 2016;17(10):1159–66.

69. Luo Y, Cai X, Liu S, Wang S, Nold-Petry CA, Nold MF, et al. Suppression of antigen-specific adaptive immunity by IL-37 via induction of tolerogenic dendritic cells. Proc Natl Acad Sci. 2014;111(42):15178–83.

70. Guttman-Yassky E, Zhou L, Krueger JG. The skin as an immune organ: Tolerance versus effector responses and applications to food allergy and hypersensitivity reactions. J Allergy Clin Immunol. 2019;S0091-6749(19):30474–9.

731 **Figure legends**

Fig. 1. BMP7-driven LCs show up-regulation of inflammation-associated genes.

(A) Schematic overview of *in vitro* LC generation from $CD34^+$ cord blood hematopoietic progenitor cells. Bright field images represent day 7 LC clusters. Flow cytometry contour plots represent day 7 expression of CD1a/CD207 induced by TGF-β1 or BMP7. **(B)** Heat map visualizes gene expression profiles of differentially expressed genes. $CD1a^+/CD207^+$ LCs were generated from three independent donors in response to TGF-β1 or BMP7 and were FACS sorted before analysis. Colors represent high (red) and low (blue) intensity. **(C)** qRT-PCR analysis of TLR1-10 mRNA expression by day 7 generated MACS sorted LCs (TGF-β1 vs. BMP7). Values are normalized to HPRT (n=4, ±SD, 2-tailed Student's t test, *P<0.05; ** P<0.005). **(D)** Flow cytometry contour plots represent day 7 expression of TLR2 on $CD207^+$LCs induced by TGF-β1 or BMP7. Graph represents mean fluorescence intensity (MFI) of TLR2 by $CD207^+$ cells (n=4, ±SD, 2-tailed Student's t test, *P<0.05). **(E)** MACS sorted LCs (TGF-β1-LCs or BMP7-LCs) were activated or not for 48h with 5µg/ml PGN and cytokine production was measured by cytokine array (right; n=3, 1-way ANOVA, corrected with Tukey multiple comparison test, * P<0.05; ** P<0.005; *** P<0.005).

Fig. 2. Immunophenotypic analysis of *in vitro* generated LCs.

(A) Pre-expanded $CD34^+$ cells were cultivated for 7 days with GM-CSF, FLT3-L, SCF, TNFα and either TGF-β1 or BMP7. Histograms depict relative expression level of indicated markers for gated $CD1a^+/CD207^+$ cells. Bars graphs represent mean fluorescence intensity (MFI) for listed markers (n=4, mean ±SD, 2-tailed Student's *t* test, * P<0.05; ** P<0.005; *** P<0.0005). **(B)** Phenotype of MACS sorted peripheral blood monocytes vs. $CD1c^+$ DCs. **(C)** $CD14^+$ peripheral blood monocytes were differentiated to LCs for 5 days with GM-CSF and either TGF-β1 or BMP7. Histograms depict relative expression level of CD1c and CD206 for gated $CD1a^+/CD207^+$ cells (n=3). **(D)** $CD1c^+$ peripheral blood DCs were differentiated to LCs for 3 days with GM-CSF and either TGF-β1 or BMP7. Histograms depict relative expression level of CD1c and CD206 for gated $CD1a^+/CD207^+$ cells (n=3). **(E)** $CD34^+$ cells-derived LCs were FACS sorted for $CD207^+$ cells, then fixed with

glutaraldehyde. Ultrathin sections were analyzed with Tecnai-20 transmission electron microscope (n=3). Size bars left = 2µm; right = 500nm**.**

Fig. 3. The psoriatic epidermis harbours LCs with phenotypical resemblance to *in vitro* BMP7-driven LCs. Representative images of sections from healthy adult human skin **(A)** and psoriatic lesions **(B)** were analyzed for the expression of CD207, CD1c and CD206. Arrow heads indicate triple positive CD207/CD1c/CD206 cells. Scatter plot (right) shows % of $CD1c^+CD206^+$ cells in $CD207^+$ population (n=3, 2-tailed Student's *t* test, *P<0.05). **(C)** Single cell suspension from biopsies of lesional skin of two psoriatic patients was analyzed with flow cytometry. After gating for singlets and viable cells, $CD207^+$ cell population has been assessed for the expression of CD1c, CD206, and TLR2. Scatter plot (right) shows % of $CD1c^+CD206^+TLR2^+$ cells in $CD207^+$ population (n=2). Representative images of sections from healthy adult human skin **(D)** and psoriatic lesions **(E)** were analyzed for the expression of BMPRII and CD207. Scatter plot (right) shows % $CD207^+$ co-expressing BMPRII (n=3). Nuclei were visualized with Dapi. The dotted lines represent the dermal–epidermal junction (n=3). Size bar=50µm.

Fig. 4. BMP7-SMAD1/5/8 signaling is strongly induced in the psoriatic epidermis. Representative images of paraffin sections from healthy adult human skin and psoriatic lesions were analysed for the expression of CD1a, BMP7 **(A, B)** and CD1a, phospho-SMAD1/5/8 (pSMAD1/5/8) **(C, D)**. Nuclei were visualized with Dapi. The dotted lines represent the dermal–epidermal junction (n=3). Size bar = 50µm. **(E)** Representative images of sections from the ears of Junf/fJunBf/f K5cre-ERT mice (ctrl – cre- litermate control, KO d7 – Jun/JunB knockout day 7, KO d12 – Jun/JunB knockout day 14) analysed for the expression of BMP7, CD207 and phospho-SMAD1/5/8 (pSmad1/5/8). Nuclei were visualized with Dapi. The dotted lines represent the dermal–epidermal junction (n=5). **(F)** Schematic presentation of noggin (nog) and tamoxifen (Tx) treatment regiment of Junf/fJunBf/f K5cre-ERT mice. **(G)** Ear swelling in control and Jun/JunB KO animals intradermaly injected with ctrl (0.1% BSA+beads) or noggin (nog+beads) n=5, ±SEM, 1-way ANOVA, corrected with Tukey multiple comparison test, * P<0.05. **(H)** Representative images of disease progression in nog (KO nog) and ctrl (KO ctrl) injected ears on experiment day 12. **(I)** Epidermal thickness in all experimental groups

assessed based on H&E staining (n=6, ±SEM, 1-way ANOVA, corrected with Tukey multiple comparison test, * P<0.05; ** P<0.005). **(J)** Ear skin histology (H&E, day 12) of control and Jun/JunB KO animals intradermally injected with ctrl (0.1% BSA) or noggin (nog). Size bar = 100µm

Fig. 5. BMP7 supplementation is associated with mitotic activity of CD207$^+$ LC.

(A) Pre-expanded CD34$^+$ cells were cultivated for 7 days with GM-CSF, FLT3-L, SCF, TNFα and either TGF-β1 or BMP7. Graph depicts proliferation (total cell number) at day 7 and day 14 (n=4, mean ±SD, 2-tailed Student's t test, ** P<0.005). **(B)** Graph represents % of phenotypically defined cells generated as stated in A, and analyzed by flow cytometry for the expression of LC lineage markers CD1a, CD207, CD324 (n=4, 2-tailed Student's t test, * P<0.05; ** P<0.005). **(C)** Immunofluorescent and immunohistochemical stainings represent sections of day 7 generated LC clusters analyzed for the expression of Ki67 and CD207. Size bar = 50µm (n=3). **(D)** % of Ki67$^+$ cells among total CD207$^+$ LCs. Each symbol represent one cluster (n=10, 2-tailed Student's t test, **** P<0.0001). **(E)** Representative images of sections from healthy adult human skin and psoriatic lesions were analyzed for the expression of BMP7, Ki67 and CD207. Nuclei were visualized with Dapi. The dotted lines represent the dermal–epidermal junction. Size bar = 50µm (n=3). **(F)** % of Ki67$^+$ LCs calculated from immunohistology sections from healthy and psoriatic skin. Each symbol represents one patient. **(G)** Pie charts depict % of CD207$^+$ cells confined to the KC layers expressing BMP7 in healthy (n=2, mean) and psoriatic skin (n=4, mean). Mean was calculated from immunohistological sections.

Fig. 6. TGF-β1 represses BMP7-driven CD206$^+$CD1c$^+$ LC characteristics via ALK5.

(A) Schematic representation of canonical TGF-β/BMP7 downstream signaling. **(B)** CD34$^+$ cells were induced to differentiate into LCs in the presence of TGF-β1 or BMP7 for 8 days. Parallel day 6 cultures were supplemented with BMP7 or TGF-β1 as indicated. Representative contour plots show expression of CD1c vs CD206 by gated day 8 generated CD1a$^+$CD207$^+$ cells. Bars represent mean fluorescence intensity (MFI) of CD1c/CD206 for gated CD1a$^+$/CD207$^+$ cells (n=3, ±SD). **(C)** CD34$^+$ cells were cultured for 4 days, then pre-treated or not with SB421543 (ALK5 inhibitor) for 1 h,

followed by TGF-β1 addition. Representative contour plots show day 7 generated gated $CD1a^{+}CD207^{+}$ cells analyzed for the expression of CD1c and CD206. Bars represent mean fluorescence intensity (MIF) of CD1c/CD206 expression by gated $CD1a^{+}/CD207^{+}$ cells pretreated or not with 8μM ALK5 inhibitor (n=3, ±SEM, 2-tailed Student's *t* test, * P<0.05; ** P<0.005).

Fig. 7. Reduction in lesional epidermal BMP7 expression in psoriasis correlates with clinical improvement. (A) Graph indicates relative staining intensity of BMP7 before and after dithranol treatment analyzed using ImageJ software (n=6, 2-tailed Student's t test, * P<0.05). Representative images of sections from the lesional skin of psoriatic patients analyzed for the BMP7 expression before and after dithranol treatment. Size bar = 50μm. **(B)** Correlation between PASI score reduction and BMP7 relative staining intensity reduction after dithranol treatment (n=6, nonparametric Sperman correlation).

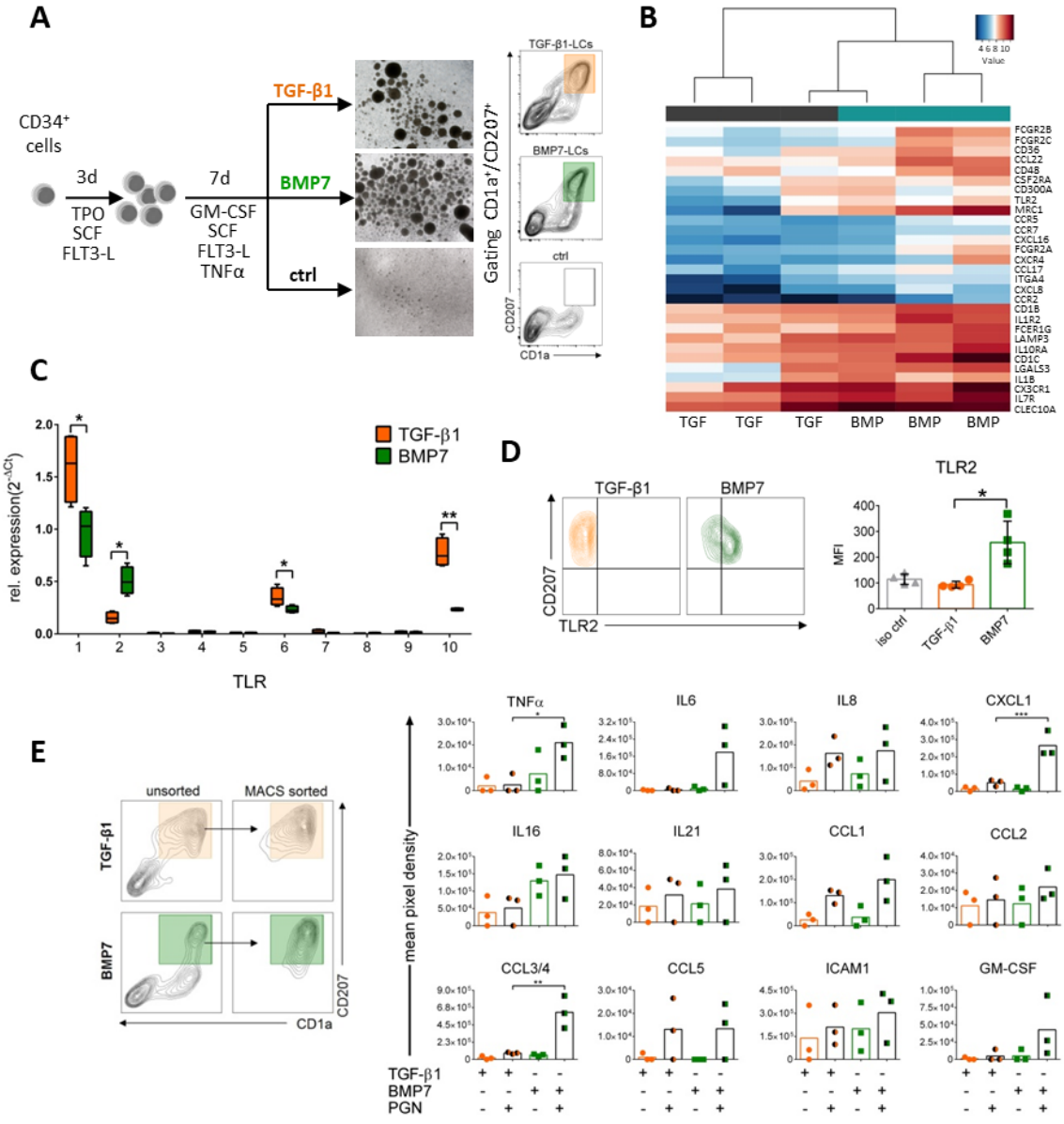
A
CD34+ cells
3d
TPO
SCF
FLT3-L
7d
GM-CSF
SCF
FLT3-L
TNFα
TGF-β1
BMP7
ctrl
TGF-β1-LCs
BMP7-LCs
ctrl
Gating CD1a+/CD207+
CD207
CD1a
B
Value
FCGR2B
FCGR2C
CD36
CCL22
CD48
CSF2RA
CD300A
TLR2
MRC1
CCR5
CCR7
CXCL16
FCGR2A
CXCR4
CCL17
ITGA4
CXCL8
CCR2
CD18
IL1R2
FCER1G
LAMP3
IL10RA
CD1C
LGALS3
IL1B
CX3CR1
IL7R
CLEC10A
TGF TGF TGF BMP BMP BMP
C
TGF-β1
BMP7
rel. expression(2-ΔCt)
TLR
D
TGF-β1
BMP7
CD207
TLR2
TLR2
MFI
iso ctrl
TGF-β1
BMP7
E
unsorted
MACS sorted
TGF-β1
BMP7
CD207
CD1a
mean pixel density
TNFα
IL6
IL8
CXCL1
IL16
IL21
CCL1
CCL2
CCL3/4
CCL5
ICAM1
GM-CSF
TGF-β1
BMP7
PGN

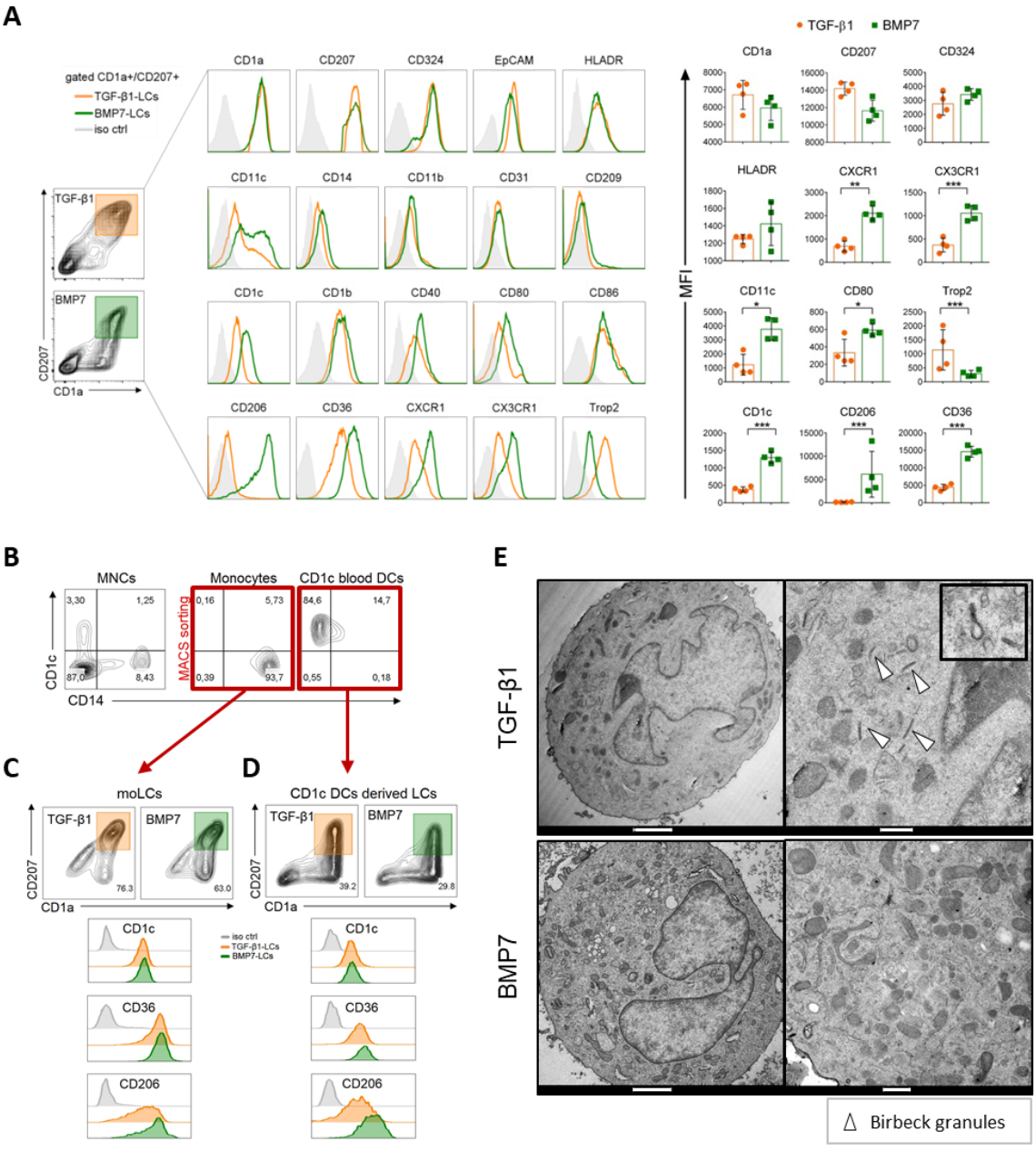
A
gated CD1a+/CD207+
TGF-β1-LCs
BMP7-LCs
iso ctrl
TGF-β1
BMP7
CD207
CD1a
CD1a
CD207
CD324
EpCAM
HLADR
CD11c
CD14
CD11b
CD31
CD209
CD1c
CD1b
CD40
CD80
CD86
CD206
CD36
CXCR1
CX3CR1
Trop2
TGF-β1
BMP7
MFI
HLADR
CXCR1
CX3CR1
CD11c
CD80
Trop2
CD1c
CD206
CD36
B
MNCs
Monocytes
CD1c blood DCs
MACS sorting
CD1c
CD14
3,30
1,25
87,0
8,43
0,16
5,73
0,39
93,7
84,6
14,7
0,55
0,18
C
moLCs
D
CD1c DCs derived LCs
TGF-β1
BMP7
CD207
CD1a
76.3
63.0
39.2
29.8
CD1c
CD36
CD206
iso ctrl
TGF-β1-LCs
BMP7-LCs
E
TGF-β1
BMP7
Birbeck granules

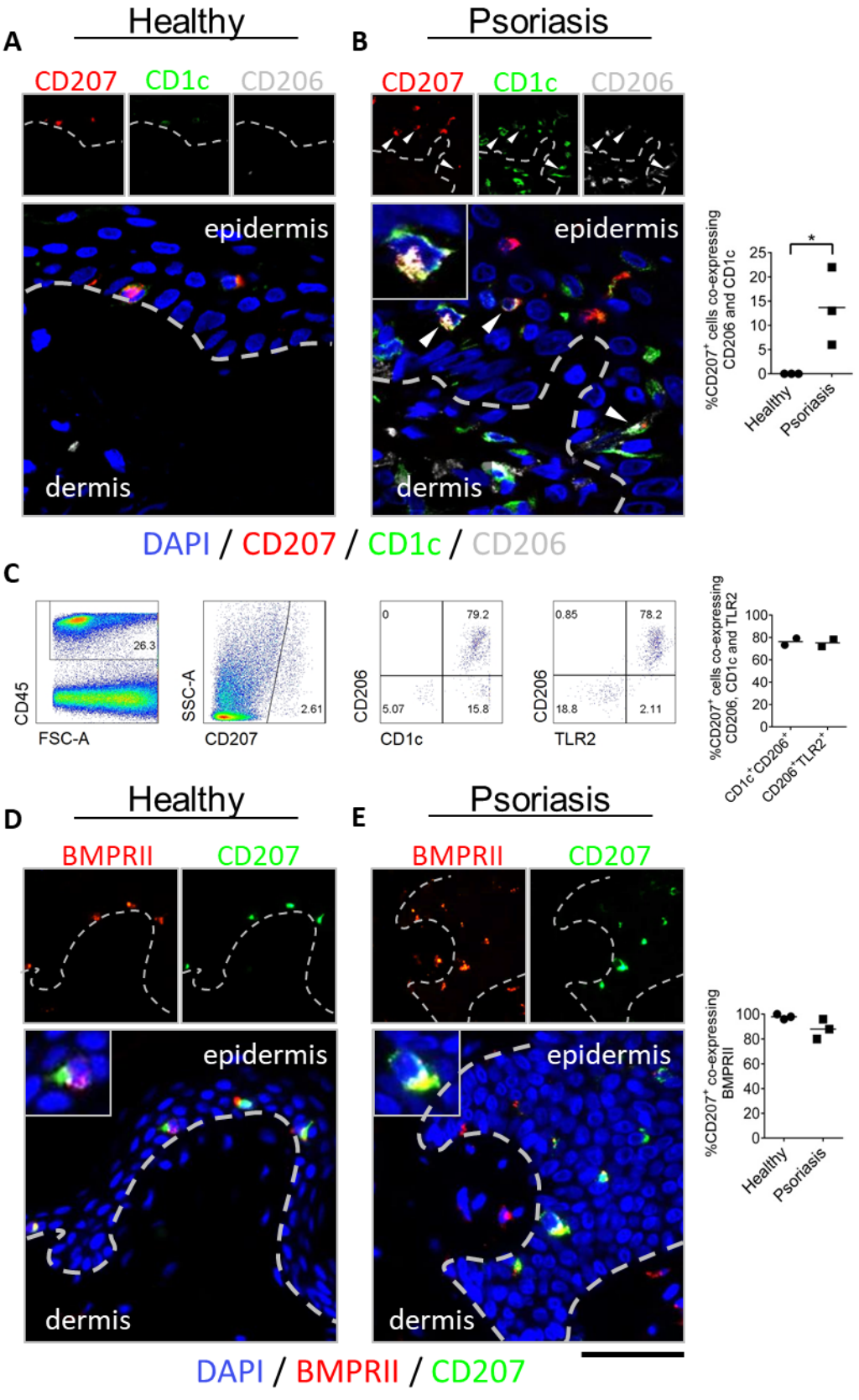
A
Healthy
B
Psoriasis
CD207
CD1c
CD206
epidermis
dermis
DAPI / CD207 / CD1c / CD206
%CD207+ cells co-expressing CD206 and CD1c
Healthy
Psoriasis
C
CD45
FSC-A
26.3
SSC-A
CD207
2.61
CD206
CD1c
0
79.2
5.07
15.8
TLR2
0.85
78.2
18.8
2.11
%CD207+ cells co-expressing CD206, CD1c and TLR2
CD1c+CD206+
CD206+TLR2+
D
Healthy
E
Psoriasis
BMPRII
CD207
%CD207+ co-expressing BMPRII

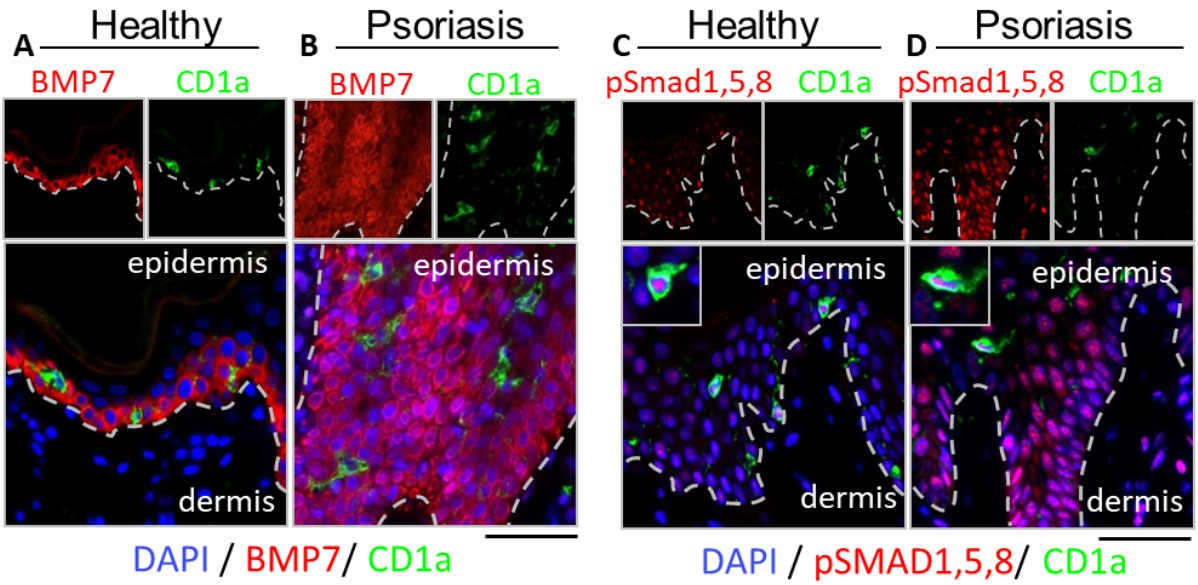
A
Healthy
BMP7
CD1a
epidermis
dermis
B
Psoriasis
BMP7
CD1a
epidermis
DAPI / BMP7/ CD1a
C
Healthy
pSmad1,5,8
CD1a
epidermis
dermis
D
Psoriasis
pSmad1,5,8
CD1a
epidermis
dermis
DAPI / pSMAD1,5,8/ CD1a

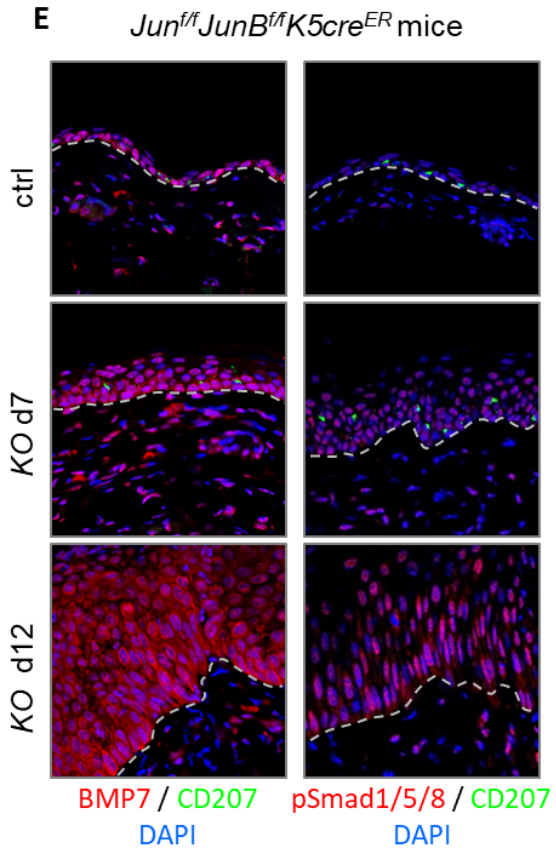
E
Jun^f/f JunB^f/f K5cre^ER mice
ctrl
KO d7
KO d12
BMP7 / CD207
DAPI
pSmad1/5/8 / CD207
DAPI

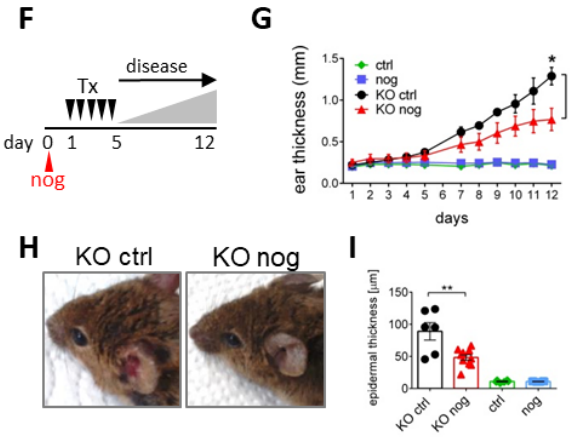
F
disease
Tx
day 0 1 5 12
nog
G
ctrl
nog
KO ctrl
KO nog
ear thickness (mm)
days
H
KO ctrl
KO nog
I
epidermal thickness [µm]
KO ctrl
KO nog
ctrl
nog

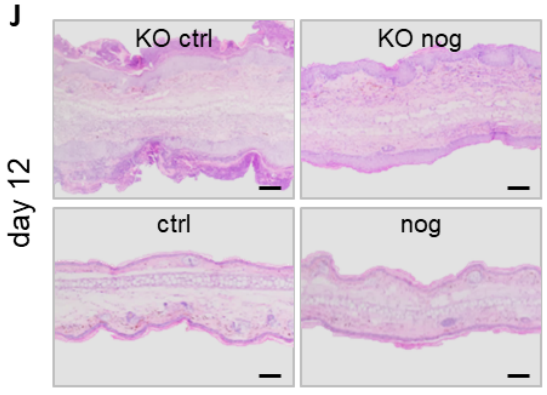
J
KO ctrl
KO nog
day 12
ctrl
nog

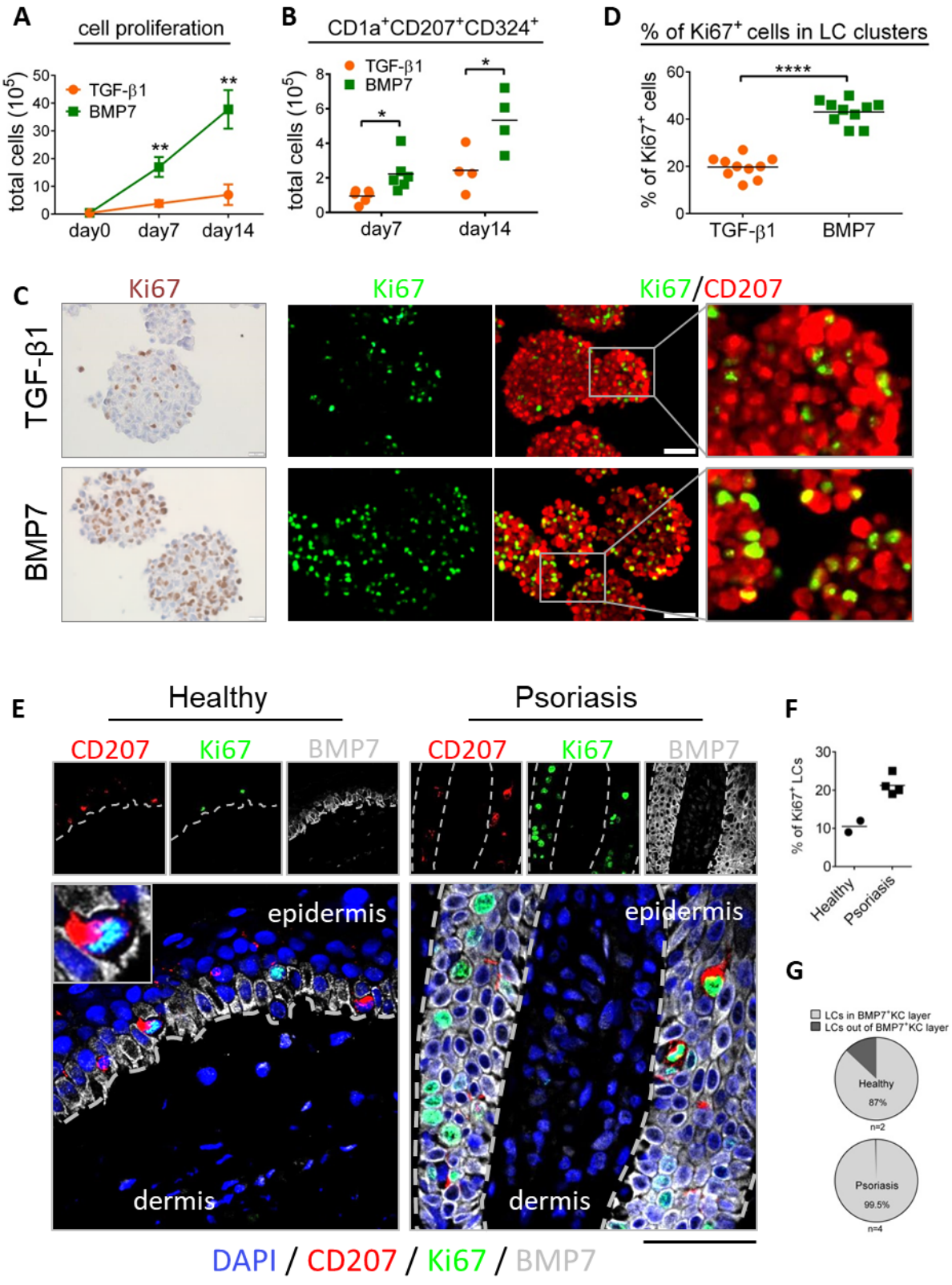
A
cell proliferation
total cells (10^5)
TGF-β1
BMP7
day0
day7
day14
B
CD1a+CD207+CD324+
total cells (10^5)
day7
day14
D
% of Ki67+ cells in LC clusters
% of Ki67+ cells
TGF-β1
BMP7
C
Ki67
Ki67
Ki67/CD207
TGF-β1
BMP7
E
Healthy
Psoriasis
CD207
Ki67
BMP7
epidermis
dermis
DAPI / CD207 / Ki67 / BMP7
F
% of Ki67+ LCs
Healthy
Psoriasis
G
LCs in BMP7+KC layer
LCs out of BMP7+KC layer
Healthy
87%
n=2
Psoriasis
99.5%
n=4

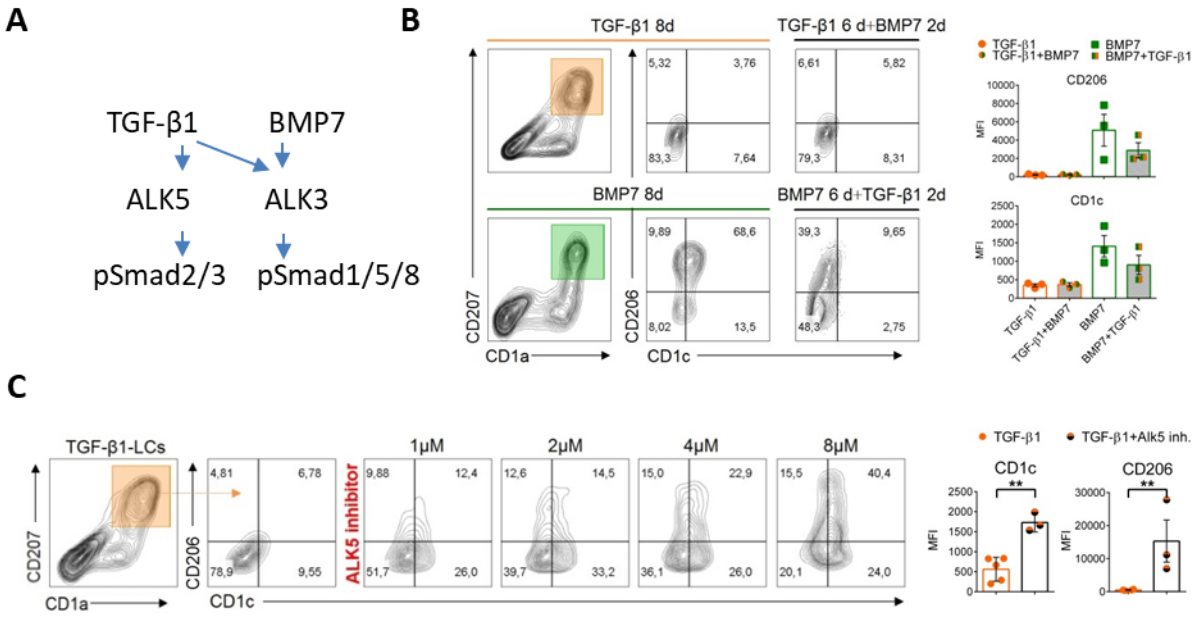

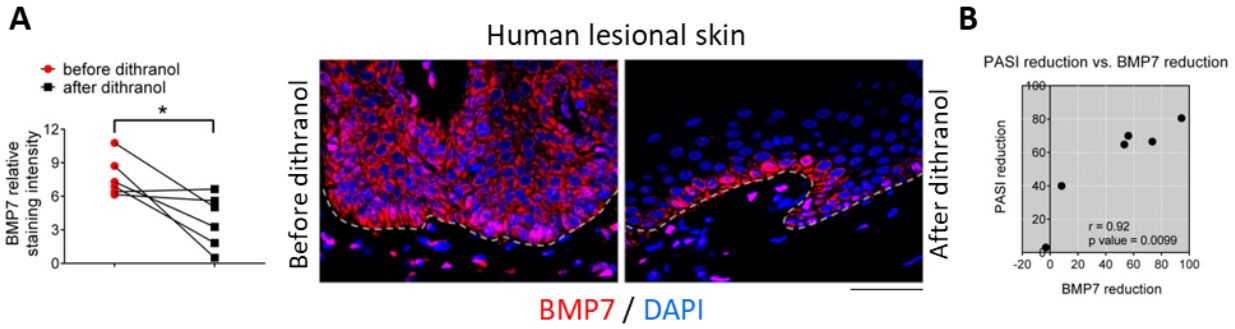

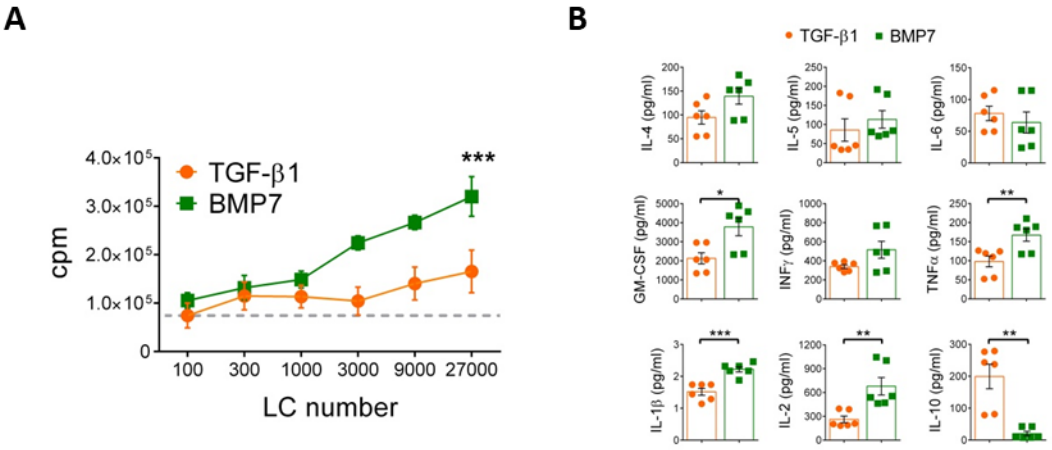

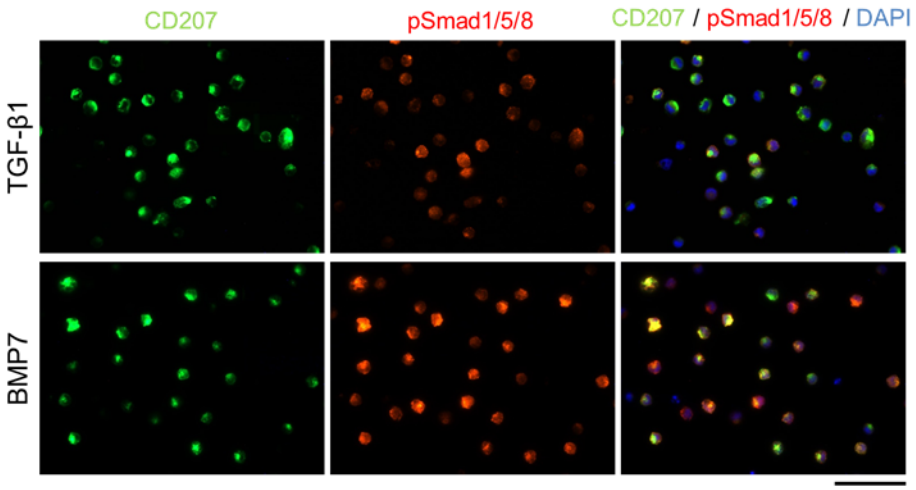

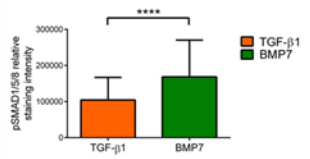

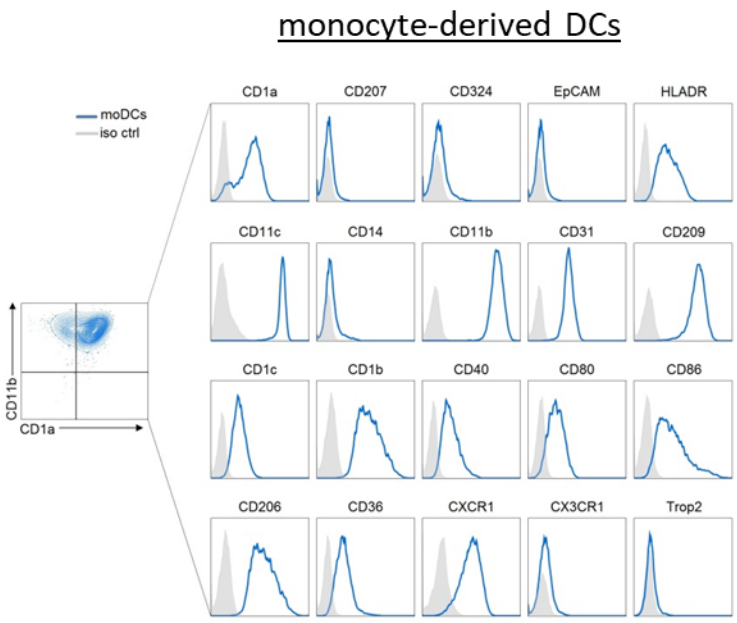

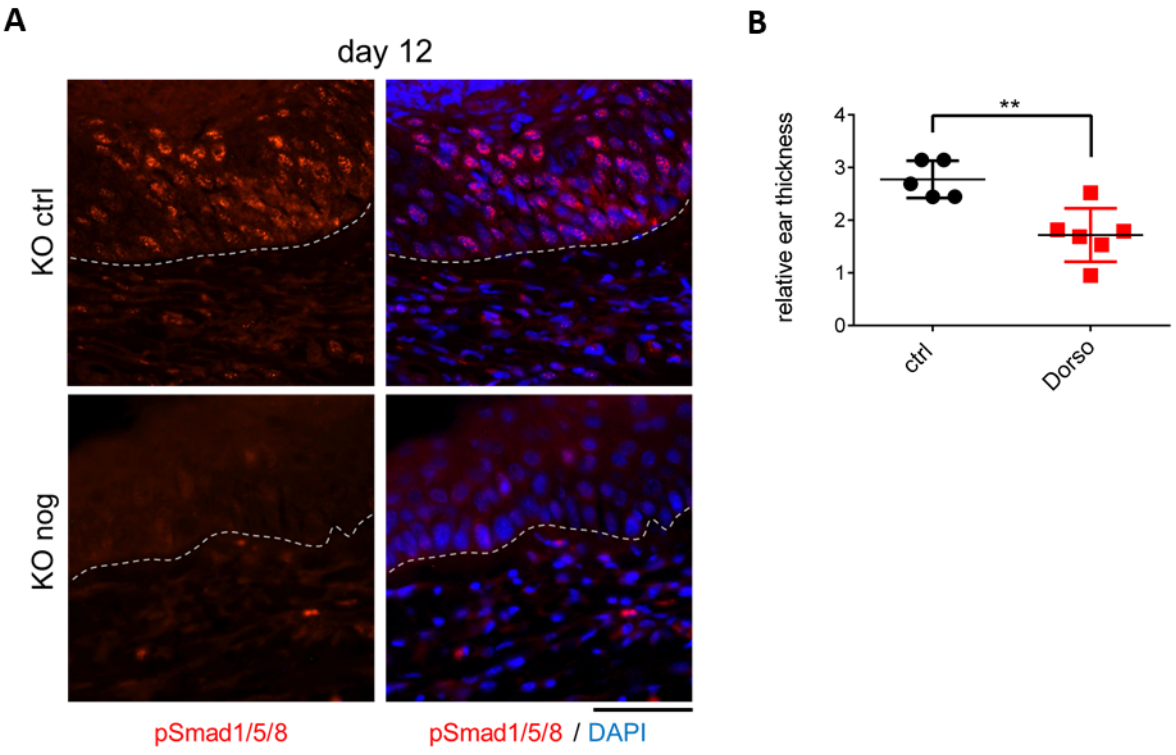

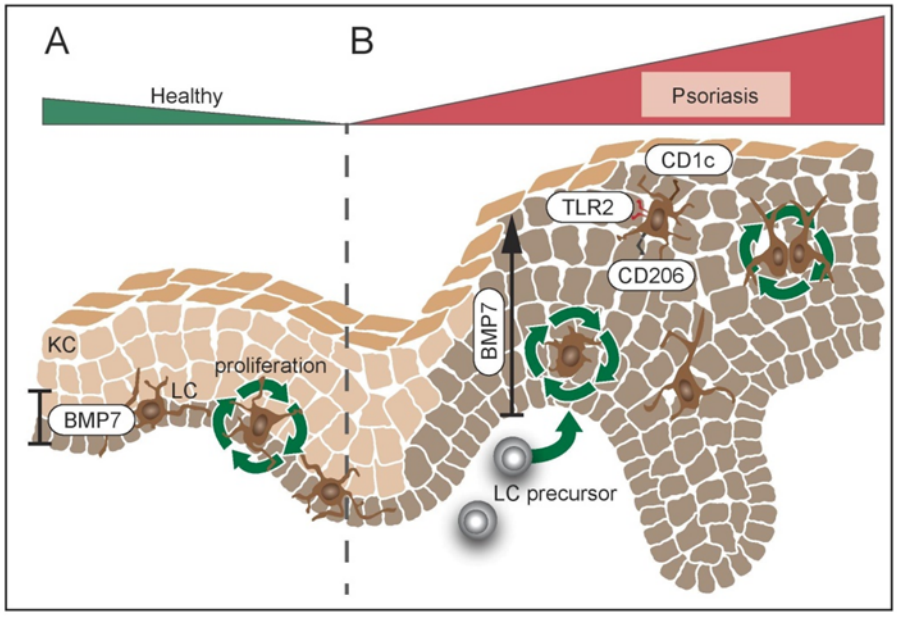
A
B
Healthy
Psoriasis
CD1c
TLR2
CD206
BMP7
KC
proliferation
LC
BMP7
LC precursor

Supplemental material

Supplementary figure legends

Supplementary methods

Supplementary tables

Table S3. qPCR primer sequences

Table S4. Immunohistology antibodies

Supplementary references

Supplementary figure legends

Fig. S1. BMP7-generated LCs exhibit immunostimulatory capacity.

(A) 10^5 naïve CD4 T cells were stimulated with the indicated numbers of LCs. Proliferation of T cells was monitored on day 5 of co-culture by addition of [methyl-3H]TdR, followed by measurement of [methyl-3H]TdR incorporation 18h later (n=3, ±SD, 2-tailed Student's t test, *** P<0.0005). **(B)** Allogeneic, naive $CD4^+$ T-cells were co-cultured for 5 days with TGF-β1- or BMP7-LCs. Cytokines in the supernatants were measured by Luminex system (n=6, ±SEM, 2-tailed Student's t test P<0.05; ** P<0.005; *** P<0.0005).

Fig. S2. BMP7-LCs express higher levels of pSmad1/5/8 than TGF-β1-LCs.

Day 7 TGF-β1- and BMP7-LCs were MACS sorted. Cytospins were immunolabeled to asses $CD207^+$ cells for the expression of pSMAD1/5/8. Graph indicates relative staining intensity of pSmad1/5/8 analyzed using ImageJ software. For the relative fluorescence intensity 150 CD207+ cells/condition were measured (n=3, 2-tailed Student's t test, **** P<0.0001).

Fig. S3. BMP7-LCs have a unique phenotype distinct from moDCs. $CD14^+$ peripheral blood monocytes were differentiated for 7 days with GM-CSF and IL-4 to moDCs. Histograms depict relative expression level of indicated markers for $CD1a^+/CD11b^+$ cell population (n=4).

Fig. S4. Inhibition of BMP signaling with noggin or Alk3 inhibitor results in decreased ear swelling *in vivo*. (A) Representative images of sections from the ears of $Jun^{f/f}JunB^{f/f}$ $K5cre\text{-}ER^T$ knock out mice injected intradermally (day 0) with beads-adsorbed noggin (KO nog) or 0.1% BSA + beads control (KO ctrl). Samples were analyzed for the expression of phospho-Smad1/5/8 (pSmad1/5/8) on day 12 of the experiment. Nuclei were visualized with Dapi. The dotted lines represent the dermal–epidermal junction (n=3). **(B)** $Jun^{f/f}JunB^{f/f}$ $K5cre\text{-}ER^T$ knock out mice were treated topically from day 10 of the experiment, with 10uM dorsomorphin (Dorso) for 5 consecutive days. Graph represents differences in ear thickness measured on day 15 (n=5-6, 2-tailed Student's *t* test, **P<0.005).

Fig. S5. Hypothetical model of pathogenic epidermal BMP signaling in psoriasis.

BMP7 is expressed aberrantly throughout all KC layers in the lesional psoriatic epidermis and promotes the generation of proliferative $CD206^{+}CD1c^{+}TLR2^{+}$LCs from precursors. These psoriatic LCs occur scattered throughout the enlarged epidermis. Conversely, in the healthy epidermis, LCs are $CD206^{-}TLR2^{-}CD1c^{low/-}$, exhibit a predominant basal/suprabasal location, and the occasionally observed mitotic LCs are confined to the basal $BMP7^{+}$ KC layer. In psoriasis, aberrantly activated canonical BMP-pSMAD1/5/8 signaling promotes lesion formation and induces the generation of inflammatory LCs, sensitized for bacterial signaling. Our data suggest that aberrant high BMP7 in psoriatic KCs is mediated by a KC intrinsic process and enhances microbial signals in psoriatic lesions.

Supplementary methods

Cell isolation

CD34$^+$ hematopoietic progenitor/stem cells (HSCs): . Cord blood was collected during healthy, full-term deliveries. Ethics approval (26-520) was obtained from the Medical University of Graz Institutional Review Board for these studies. Informed consent was provided to patients in accordance with the Declaration of Helsinki. Cord blood CD34$^+$ HSCs were positively selected with magnetic sorting (EasySep™ Human CD34 Positive Selection Kit, StemCell Technologies™). CD14$^+$ monocytes, naive CD4$^+$ T-cells, CD1c$^+$ blood DCs: Buffy coats from healthy donors were purchased from Transfusion Medicine Department, Medical University of Graz, Austria. For the isolation of peripheral blood mononuclear cells (PBMCs) heparinized blood was separated by gradient centrifugation with Lymphoprep™ (Axis Shield, Norway). Subsequently, various cells were isolated using magnetic sorting technique according to the manufacturer's instructions. First, CD14$^+$ monocytes were positively selected (CD14 MicroBeads, human, Miltenyi Biotec, Germany). Second, after depletion of CD19$^+$ cells, CD1c$^+$ blood dendritic cells were positively selected (CD1c$^+$/BDCA-1 Dendritic Cell Isolation Kit, human, Miltenyi Biotec, Germany). Last, naïve CD4$^+$ T-cells were negatively selected (MagniSort™ Human CD4 Naïve T cell Enrichment Kit, ThermoFisher Scientific, USA). Purity of sorted cells was assessed by flow cytometry and was greater than 95%.

Preparation of single cell suspension from psoriatic skin biopsies

Punch biopsies (4 mm) have been taken from lesional skin of psoriatic patients. Ethics approval (EK700/2009) was obtained from the Medical University of Vienna Institutional Review Board for these studies. Informed consent was provided to patients in accordance with the Declaration of Helsinki. To prepare single cell suspension gentleMACS™ Dissociator (Miltenyi Biotec, Germany) have been used. Skin biopsy was cut into small pieces and transferred into gentleMACS C Tube (Miltenyi Biotec, Germany) containing mix of 900 µl Collagenase IV (0.5 Wünsch units/ml) and 100 µl DNAse I (10 mg/ml). Tissue with enzymes was incubated overnight in 37°C in shaking water bath. This was followed by tissue disassociation using gentleMACS™ Dissociator system. Obtained cell

suspension was filtered through 100 µm cell strainer and centrifuged for 10 min in 4°C at 1600 rpm. After supernatant was discarded cell pellet was stained for flow cytometry analysis.

Gene expression analysis

The raw data of the dataset GSE49085 (1) (6 samples, Affymetrix Human Genome U133 Plus 2.0 Array) was downloaded from Gene Expression Omnibus (2) and analysed in R 3.5.1 (https://www.R-project.org). The R package 'oligo' (3) was used for quality control and pre-processing. The R package 'limma' (4) was used to calculate log2 (fold changes) and p values between the groups with patients as covariates. Specific filtering was applied using selected features associated with dendritic cells (24). The p-values were adjusted for multiple testing with Benjamini and Hochberg's method to control the false discovery rate. Genes with an absolute $\log_2$(fold change) > log2(1.5) and an adjusted p-value <= 0.05 were considered as differentially expressed. Hierarchical clustering with Euclidean distance and Ward linkage was performed and visualized as a heatmap. The heatmap was generated using the R package 'gplots'.

RNA isolation, reverse transcription (RT-PCR) and real-time quantitative PCR (qPCR)

Prior to the RNA extraction, day 7 $CD207^+$ cells were isolated with magnetic sorting (human CD207/Langerin MicroBeads, Miltenyi Biotec, Germany). Extraction of total RNA from sorted LCs (purity ≥ 80%) was performed with RNeasy Micro Kit (Qiagen, Germany). cDNA was generated using High-Capacity cDNA Reverse Transcription Kit (Applied Biosystems, USA). The qPCR was performed using Fast SYBR™ Green Master Mix (Applied Biosystems, USA) and CFX96 Real-Time Thermal cycler (Bio-Rad Laboratories, USA). All steps were performed according to the manufacturer's instructions. Values were normalized to HPRT. Primer sequences are listed in the supplementary table 2.

Cytokine measurements

Day 7 $CD207^+$ LCs (TGF-β1-LCs vs. BMP7-LCs) were MACS sorted (purity ≥90%) and activated with 5 µg/ml PGN. After 48h supernatants were collected. The proteome profiler human cytokine array kit (R&D Systems, USA) was used according to the manufacturer's instructions. Spot intensity

was quantified with ImageLab™ software (BioRad). For the quantitative measurement of cytokines in the supernatants from T-cell/LC co-culture experiments Luminex system was used.

Transmission electron microscopy (TEM)

Day 7 FACS sorted $CD207^+$ LCs were fixed with 2,5% Glutaraldehyde and 1% OsO4 palade and dehydrated in a graded ethanol series. Afterward, LCs were embedded in Epon (Serva, Germany) and ultrathin sections (70–100 nm) were cut using an UltraCut-UCT ultramicrotome (Leica Inc., Austria), transferred to copper grids, and viewed either unstained or stained with 1% uranyl acetate and 5% lead citrate (Merck, Germany) using a Tecnai-20 TEM (Tecnai-20 equipped with a LaB6 cathode; FEI Company, Netherlands) at an acceleration voltage of 80 kV. Digital images were recorded with an Eagle 4 k-CCD camera; chip size: 4,096 × 4,096 pixels (FEI Company).

Immunofluorescence and immunohistochemistry

Healthy, adult (18-42 year) skin samples were collected after plastic surgery. Ethics approval (27-071) was obtained from the Medical University of Graz Institutional Review Board for these studies. Informed consent was provided to patients in accordance with the Declaration of Helsinki. Paraffin sections (4µm) were subjected to HIER antigen retrieval in Target Retrieval Solution pH 6.0 (Agilent/Dako, USA) followed by blocking with 5% donkey serum (Jackson ImmunoResearch Laboratories, USA). Primary and secondary antibodies are listed in the supplementary table 4. Staining specificity controls were performed with substitution of primary antibodies by isotype-matched control antibody against irrelevant antigens followed by corresponding secondary antibody. To visualize nuclei, sections were counterstained with 10µg/mL DAPI. Images were obtained with Leica DM4000B microscope and ZEIS LSM700 confocal microscope and processed using LAS V3.8, ZEN 2.3 lite, and ImageJ software.

Mice

$Jun^{f/f}JunB^{f/f}$ K5cre-ER^T mice (mixed background) with conditional deletion of Jun/JunB under keratin 5 promoter (K5cre-ERT) were described previously (5). To delete Jun/JunB K5-cre^{ER} positive (KO) or negative (ctrl; $Jun^{f/f}JunB^{f/f}$) mice were injected intraperitoneally with 1 mg tamoxifen (Tx, Sigma-

Aldrich, USA) in an emulsion with sunflower seed oil (Sigma-Aldrich)/ethanol mixture (10:1) on 5 consecutive days. Deletion of Jun/JunB was verified by PCR. Mice were kept in the animal facility of the Medical University of Vienna in accordance with institutional policies and federal guidelines. Animal experiments were approved by the Animal Experimental Ethics Committee of the Medical University of Vienna and the Austrian Federal Ministry of Science and Research. (Animal license numbers: GZ 66.009/124-BrGT/2003; GZ 66.009/109-BrGT/2003; BMWF-66.009/0073-II/10b/2010 BMWF-66.009/0074-II/10b/2010; BMWFW-66.009/0200-WF/II/3b/2014; and BMWF W-66.009/0199-WF/II/3b/2014).

Intradermal noggin injections in mice

For delivery of Noggin-adsorbed beads, we used a previously described approach (6–9). Ears of *Jun$^{f/f}$JunB$^{f/f}$ K5cre-ER^{T}* mice were injected intradermally one time with a mix of FluoSpheres® (Invitrogen, USA) and noggin (300ng) 24h before Tx injection. For control challenge injection a mix of FluoSpheres® and 0.1% BSA was used.

Topical treatment with dorsomorphin

Jun$^{f/f}$/JunB$^{f/f}$K5-cre-ER^{T} mice aged 5-6 weeks were injected with Tamoxifen (Tx) to trigger psoriasis as previously published (5,10) After five consecutive days of Tx injection, mice were given an additional 5 days to manifest a pronounced phenotype. After this, for another five consecutive days inhibitors were applied topically to the ears of the mice. Dorsomorphin (Tocris Bioscience, UK) was diluted to a concentration of 10µM in DMSO; of this mixture, 40µL were pipetted onto each mouse ear (20µl to the dorsal, 20µl to the ventral side). The control group received pure DMSO. Ear thickness was measured daily via caliper. After five days of treatment (from day 10 to 15), the increase of ear thickness relative to ear thickness at the start of inhibitor treatment was calculated.

Murine skin thickness measurement

Paraffin sections from mouse ears were stained with hematoxylin and eosin (Sigma, USA). Images were obtained with Olympus BX53 (Olympus) microscope. Epidermal thickness was measured in 20

random fields on 5 independent pictures per sample (magnification 10x) using AxioVision LE64 software (Zeiss).

T-cell proliferation assay (MLR)

The assay was performed as described previously (11). In brief, MACS-sorted $CD207^+$ LCs were seeded in graded numbers with a constant number ($5x10^5$) of purified, allogenic naive $CD4^+$ T-cells in 96-well tissue culture plates in RPMI-1640 medium (Sigma-Aldrich, USA) supplemented with 10% FBS. The proliferation of T-cells was analyzed on day 5 of culture by adding [methyl-^{3}H]TdR followed by incorporation measurement [methyl-^{3}H]TdR 18h later. Incorporated radioactivity was measured using a 1450 microbeta plate reader (Wallac-Trilux Instrument; Life Science). Supernatants were collected for cytokine measurement (Luminex) before adding [methyl-^{3}H]TdR. Assays were performed in triplicates.

Supplementary tables

Antibody (anti-)	Clone	Company
CD1a	HI149	BD Biosciences
CD1b	SN13(K5-1B8)	BioLegend
CD1c	510/21A3	BD Biosciences
CD11b	ICRF44	BioLegend
CD11c	BU15	BioLegend
CD14	M5E3	BioLegend
CD31	WM59	BioLegend
CD36	CB38	BD Biosciences
CD40	5C3	BD Biosciences
CD80	L307.4	BD Biosciences
CD86	2331(FUN-1)	BD Biosciences
CD206	15-2	BioLegend
CD207	DCGM4	Beckman Coulter
CD209	eB-h209	eBioscience
CD324/E-cadherin	67A4	BD Biosciences
CXCR1	8F1-CXCR1	BioLegend
CX3CR1	2A9-1	eBioscience
HLADR	G46-6	BD Biosciences
EpCAM/Trop1	EBA-1	BD Biosciences
Trop2	162-46	BD Biosciences
TLR2	1167	BD Biosciences

Table S1. Flow cytometry antibodies

Cytokine/reagent	Company
Trombopoietin (TPO)	PeproTech, UK
Stem cell factor (SCF)	
Fms-related tyrosine kinase 3 ligand (FLT3-L)	
Tumor necrosis factor alpha (TNFα)	
Granulocyte-macrophage colony-stimulating factor (GM-CSF)	
Interleukin 4 (IL-4)	
Transforming growth factor beta 1 (TGF-β1)	R&D Systems, USA
Recombinant mouse noggin (NOG)	
Bone morphogenetic protein 7 (BMP7)	ImmunoTools, Germany
Alk4/5/7 inhibitor (SB431542)	Tocris Bioscience, UK
Dorsomorphin	
FluoSpheres® carboxylate-modified microspheres 0.2 µm, crimson fluorescent (625/645) 2% solids	Invitrogen, USA
Recombinant extracellular domain of Notch ligand Delta-1 (Delta-1^{ext}–IgG)	Kindly provided by I. Bernstein

Table S2. Cytokines and reagents

Name	Orientation	Sequence 5'→3'
TLR1	fw	GGCACCCCTACAAAAGGAATC
	rev	TGAAGATAATGGCAAAATGGAAG
TLR2	fw	GCTGCCATTCTCATTCTTCTG
	rev	GCCACTCCAGGTAGGTCTTG
TLR3	fw	TCCACCACCAGCAATACAAC
	rev	AAGCCAAGCAAAGGAATCG
TLR4	fw	TCATTGTCCTGCAGAAGGTG
	rev	AGATGTTGCTTCCTGCCAAT
TLR5	fw	TTGCTCAAACACCTGGACAC
	rev	CACCACCATGATGAGAGCAC
TLR6	fw	GACCTACCGCTGAAAACCAA
	rev	CTCACAATAGGATGGCAGGA
TLR7	fw	TCCTAAAACTCTGCCCTGTGA
	rev	GGGAGATGTCTGGTATGTGG
TLR8	fw	GGGGATCAAAGAGGGAAGAG
	rev	TTGGGATGTGGAAAGAGACC
TLR9	fw	CTGCCTTCCTACCCTGTGAG
	rev	AGAATCATGGAGGTGGTGGA
TLR10	fw	TGGTTGGATGGTCAGATTCA
	rev	AGGGCAGATCAAAGTGGAGA
HPRT	fw	GACCAGTCAACAGGGGACAT
	rev	AACACTTCGTGGGGTCCTTTTC

Table S3. qPCR primer sequences

pAb – polyclonal antibody
mAb – monoclonal antibody

Primary antibody	Clone	Company
pAb rabbit anti-CD207	N/A	Sigma-Aldrich, USA
mAb rat anti-CD207 Alexa Fluor-488	929F3.01	Dendritics, France
pAb rabbit anti-BMP7	N/A	LifeSpan BioSciences, USA
mAb mouse anti-Ki67	MIB-1	Dako, USA
pAb rabbit anti-pSMAD1/5/8	N/A	CellSignaling, USA
mAb mouse anti-CD1a	O10	Novus Biologicals, USA
mAb mouse anti-CD1c	OTI2F4	Abcam, UK
pAb rabbit anti-CD206	N/A	Sigma-Aldrich, USA
pAb rabbit anti-BMPR2	N/A	
Secondary antibody (conjugated)		
pAb donkey anti-mouse DyLight488	N/A	Jackson ImmunoResearch Laboratories, USA
pAb donkey anti-mouse Cy3	N/A	
donkey anti-rabbit Cy3	N/A	
donkey anti-rabbit DyLight488	N/A	
donkey anti-rabbit Alexa Fluor-647	N/A	

Table S4. Immunohistology antibodies

Supplementary references

1. Yasmin N, Bauer T, Modak M, Wagner K, Schuster C, Köffel R, et al. Identification of bone morphogenetic protein 7 (BMP7) as an instructive factor for human epidermal Langerhans cell differentiation. J Exp Med. 2013;210(12):2597–610.
2. Edgar R, Domrachev M, Lash AE. Gene Expression Omnibus: NCBI gene expression and hybridization array data repository. Nucleic Acids Res. 2002;30(1):207–10.
3. Carvalho BS, Irizarry RA. A framework for oligonucleotide microarray preprocessing. Bioinformatics. 2010;26(19):2363–7.
4. Ritchie ME, Phipson B, Wu D, Hu Y, Law CW, Shi W, et al. Limma powers differential expression analyses for RNA-sequencing and microarray studies. Nucleic Acids Res. 2015;43(7):e47.
5. Zenz R, Eferl R, Kenner L, Florin L, Hummerich L, Mehic D, et al. Psoriasis-like skin disease and arthritis caused by inducible epidermal deletion of Jun proteins. Nature. 2005;437(7057):369–75.
6. Plikus M V, Mayer J, Cruz D De, Baker RE, Maini PK, Maxson R, et al. Cyclic dermal BMP signaling regulates stem cell activation during hair regeneration. Nature. 2008;451(7176):340–4.
7. Greco V, Chen T, Rendl M, Schober M, Pasolli HA, Stokes N, et al. A Two-Step Mechanism for Stem Cell Activation during Hair Regeneration. Cell Stem Cell. 2009;4(2):155–69.
8. Oshimori N, Fuchs E. Paracrin TGF-beta signaling Counterbalance BMP-mediated Repression in Hair Folicle Stem Cell Activation. Cell Stem Cell. 2012;10(1):63–75.
9. Lee J, Kang S, Lilja KC, Colletier KJ, Scheitz CJF, Zhang Y V, et al. Signalling couples hair follicle stem cell quiescence with reduced histone H3 K4/K9/K27me3 for proper tissue homeostasis. Nat Commun. 2016;7:11278.
10. Glitzner E, Korosec A, Brunner PM, Drobits B, Amberg N, Schonthaler HB, et al. Specific roles for dendritic cell subsets during initiation and progression of psoriasis. EMBO Mol Med. 2014;6(10):1312–27.
11. Stöckl J, Vetr H, Majdic O, Zlabinger G, Kuechler E, Knapp W. Human major group rhinoviruses downmodulate the accessory function of monocytes by inducing IL-10. J Clin

348 Invest. 1999;104(7):957–65.

349